Economic costs of heat-induced reductions in worker productivity due to global warming

Anton Orlov, Jana Sillmann, Kristin Aunan, Tord Kjellstrom, Asbjørn Aaheim

Abstract

We assess economic costs of heat-induced reductions in worker productivity at global scale under RCP2.6 and RCP8.5. Losses in worker productivity are calculated by using an empirically estimated epidemiological exposure-response function, and the associated economic costs are assessed by using a dynamic multi-region, multi-sector computable general equilibrium model. Autonomous mechanisation of outdoor work in agriculture and construction is implemented in the model. We find that under RCP8.5 by 2100, heat-induced reductions in worker productivity result in an average decline of 1.4% in global gross domestic product (GDP) relative to the reference scenario with no climate change. This is approximately 0.4 percentage points less than when no autonomous mechanisation is assumed. For comparison, measuring the economic costs using occupational health and safety recommendations leads to a 2.4% reduction in global GDP, which is substantially larger than when the epidemiological exposure-response function is used. Countries of Africa, South-East Asia, and South Asia are the worst affected by heat stress. However, economic costs could be substantially alleviated if a 2°C global warming target is achieved. Under RCP2.6, the average reduction in global GDP is only 0.5%. A large fraction of global mitigation costs of achieving the 2°C global warming target could be offset by the avoided adverse impacts of heat stress on worker productivity at higher warming levels.

Keywords: heat stress; worker productivity; cost; CGE model

1. Introduction

It is well established that heat stress (HS) can have adverse impacts on human health; extreme heat may cause heat stroke, heat exhaustion, and dehydration and worsen cardiovascular and kidney diseases (Kovats and Hajat, 2008; Blois et al., 2015). Growing scientific evidence indicates that the frequency, intensity, and duration of heat waves tend to increase with global warming (Meehl and Tebaldi, 2004; Russo et al., 2017; Dosio et al., 2018). Several empirical studies explored the relationship between HS and mortality and morbidity and showed that climate change could significantly increase the risk of heat-induced mortality and morbidity in the future (Ahmadalipour and Moradkhani, 2018; Basu and Samet, 2002; Gasparrini et al., 2017; Hajat and Kosatsky, 2010; Phung et al., 2016; Turner et al., 2012).

Furthermore, working in a hot environment increases the heat-related risk to human health because physical activities raise the metabolic heat inside the body (Parsons, 2014). Heat stress and strain depend on several factors, such as air temperature, radiated heat, humidity, wind speed (or air movement over skin), clothing, and metabolic heat generated by physical activities (Kjellstrom et al., 2009, 2016). HS may cause workplace injuries (Tawatsupa et al., 2013; Ma et al., 2019). To mitigate the heat-related risk to human health, the International Organisation for Standardisation (ISO) and the U.S. National Institute for Occupational Safety and Health (NIOSH) developed protective guidelines (standards). In essence, these standards describe the required frequency and duration of rest breaks at work during physical activities at certain heat levels. To assess the impacts of HS on work capacity, the ISO and NIOSH guidelines were used as a heat assessment metric in several impact studies (Kjellstrom et al., 2009; Dunne et al., 2013; Bröde et al., 2018). Overall, the research on heat-induced impacts on worker productivity is still at an early stage, and there is little detailed knowledge on how HS could affect the actual efficiency of work and production. However, the underlying physiological limits are well understood (Parsons, 2014), and increasing HS in workplaces due to climate change will increase the risk to human health and worker productivity (Kjellstrom et al., 2009). Several impact studies showed that economic costs due to HS may be substantial (Kjellstrom et al., 2019; Orlov et al., 2019; Roson and van der Mensbrugghe, 2012; Takakura et al., 2018, 2017). It has been shown that economic costs arising from decreased worker productivity are larger than any other climate related impacts (DARA, 2012; Hsiang et al., 2014). However, the number of economic studies remains limited, and all existing studies reveal large uncertainties in the estimates. Moreover, most of previous studies use the ISO and NIOSH standards to calculate the impacts of HS on work capacity, which implies that the estimated economic costs should be interpreted as the cost, in terms of reduced work hours and thereby production, of preventing heat-induced diseases. Yet, HS could reduce the efficiency of work (i.e., worker productivity) and this type of impact differs from the impact calculated by using the ISO and NIOSH preventative standards (Takakura et al., 2017).

In contrast to previous economic studies that analysed the cost of preventing heat-induced illness, we use the empirically estimated epidemiological exposure-response function developed by Kjellstrom et al. (2018) and Bröde et al. (2018) to assess economic costs resulting from heat-induced reductions in worker productivity at global scale under different mitigation projections. We also investigate the relevance of socioeconomic and modelling uncertainties. While previous studies assumed the same and constant level of work intensity among regions, we differentiate sectoral work intensities by regions and implement autonomous mechanisation of outdoor work in the economic model. Moreover, this study addresses the challenges of integrating spatiotemporal physical responses into a macro-economic model. The remainder of the paper is as follows. Section 2 describes the methodology. Section 3 presents and discusses the results from an economic impact assessment. The final section concludes the study.

2. Methods

To assess economic implications of heat-related impacts on worker productivity, we use an interdisciplinary approach that combines climate projections, epidemiological findings, and economic analyses. The analysis procedure is illustrated in Fig. 1. In short, climate projections on air temperatures, relative humidity, wind speed, and solar radiation are used to calculate the wet bulb globe temperature (WBGT), which is then combined with exposure-response functions to estimate the heat-induced impacts on work capacity loss (i.e., a physiological variable). Finally, the calculated losses in work capacity, which can also be interpreted as worker productivity losses or work efficiency losses (i.e., an economic variable), are implemented in a computable general equilibrium (CGE) model to investigate economy-wide impacts of HS under RCP2.6 and RCP8.5 and different socio-economic assumptions.

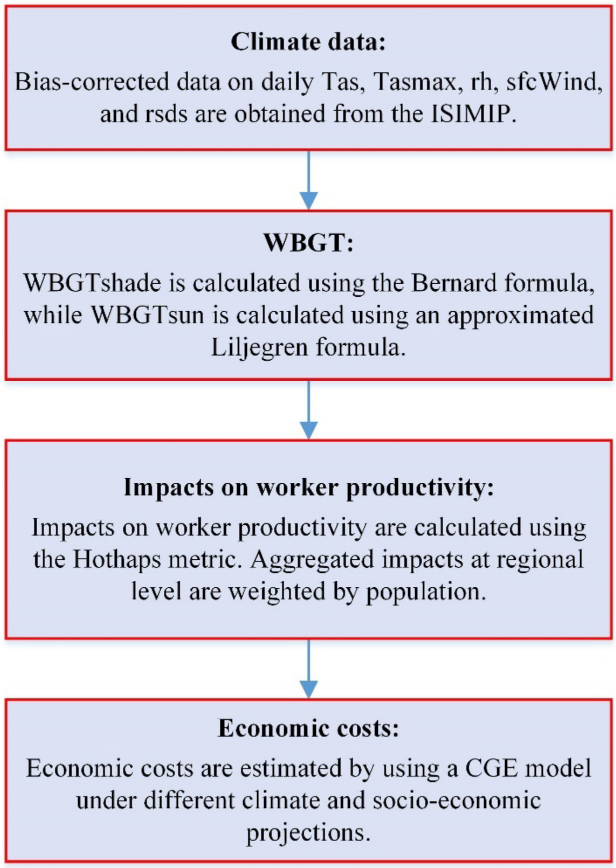

Fig. 1: Approaches and analysis procedures. *Tas* stands for daily mean temperatures, *Tasmax* is daily maximum temperatures, *rh* is relative humidity, *sfcWind* is wind speed, and *rsds* is solar radiation. *WBGTshade* stands for the WBGT indoors (or outdoor in the shadow) and *WBGTsun* is the WBGT outdoors.

2.1 Climate projections

To calculate the WBGT, we use historical and projected climate simulations from the Inter-Sectoral Impact Model Intercomparison Project (ISIMIP) (Warszawski et al., 2014), which provides bias-corrected data on daily near-surface maximum and mean temperatures, relative humidity, wind speed, solar radiation at a resolution of 0.5°×0.5° geographic grid (Hempel et al., 2013). The period from 1981 to 2005 is defined as a historical reference period, which aims to represent the current climatic conditions. For our economic impact assessment, we take climate projections associated with the representative concentration pathways, RCP2.6 and RCP8.5, which illustrate an optimistic and pessimistic scenario in terms of global warming, respectively. To investigate climate uncertainties, we use climate projections from two climate models (i.e., general circulation models (GCMs)), which are GFDL-ESM2M and HadGEM2-ES. These two models are often quoted, and envelope well the uncertainties of the ensemble-mean of the IPCC projections.

2.2 Calculation of WBGT

While there are many different heat stress indicators, WBGT is mainly used as a HS index in occupational health to measure the exposure-response relationship between climate variables and work performance. To calculate the indoor (or outdoor in the shadow) WBGT

(WBGTshade) without air conditioning, we use the formula from Lemke and Kjellstrom (2012), which was based on the formulation from Bernard and Pourmoghani (1999). This formula applies only at a wind speed of 1m/s and no heat radiation. Eq. 2.2.1 shows the core formula for the calculation of WBGTshade.

$$WBGTshade = 0.67 * Tpwb + 0.33 * Tas \qquad \text{(Eq. 2.2.1)}$$

where *Tpwb* is the psychrometric wet bulb temperature (°C), and *Tas* is the air temperature (°C).

Tpwb is calculated by using *Tas* and dewpoint temperatures by iterations, and the dewpoint temperature is calculated by using *Tas* and relative humidity. For more details regarding the calculation of *Tpwb*, we refer to Lemke and Kjellstrom (2012) and Bernard and Pourmoghani (1999). To calculate WBGTshade for each grid cell, we use an R package written by Casanueva (2019).

An accurate calculation of outdoor WBGT (WBGTsun) is more complicated than WBGTshade because it also includes the effect of wind and solar radiation. The formulas of Liljegren et al. (2008) (hereafter: the Liljegren approach) have proved to be the most accurate method to calculate WBGTsun (Lemke and Kjellstrom, 2012). Eq. 2.2.2 shows the basic formula for calculation of WBGTsun (Lemke and Kjellstrom, 2012; Liljegren et al., 2008):

$$WBGTsun = 0.7 * Tnwb + 0.2 * Tg + 0.1 * Tas \qquad \text{(Eq. 2.2.2)}$$

where *Tnwb* stands for the natural wet bulb temperature (°C) and *Tg* is the globe temperature (°C). More details on the calculation of *Tnwb* and *Tg* can be obtained from Liljegren et al. (2008).

The Liljegren approach also requires iterative solutions, which are very computationally intensive, especially for data with a high spatiotemporal resolution. In essence, the calculation of WBGTshade and WBGTsun is formulated as a non-linear optimisation problem. The calculation of WBGTsun using the Liljegren approach is much more computationally intensive than the calculation of WBGTshade because one has to consider latitude, the month, and the time of day (i.e., azimuth of the sun) to obtain a correct solar radiation. Therefore, we approximate the Liljegren approach as follows. First, using the ISIMIP daily data on temperatures, solar radiation, and wind speed over the period of 2011-2020, we calculated the WBGTsun using the Liljegren approach. Then, we conduct a regression analysis, where the response variable is the calculated WBGTsun and the explanatory variables are air temperatures, dewpoint temperatures, solar radiation, wind speed, month, and latitude. Finally, we perform an out-of-sample validation. We find that a 2nd order polynomial provides a very good approximation with a high accuracy. We use the estimated polynomial to calculate the WBGTsun for the entire datasets. For more details, see the supplementary material, SM1.

In our analysis, both WBGTshade and WBGTsun are calculated on a daily basis and for each grid cell for the historical reference period in both RCP2.6 and RCP8.5. Working hours differ by economic sector, but core hours typically vary from 6am to 6pm. Temperatures vary within a day, and so do the heat-induced impacts on worker productivity. Future projections of climate variables are not available on an hourly basis in ISIMIP. To calculate average daily impacts, we use an approximation for hourly data based on the 4+4+4 method implemented by Kjellstrom et al. (2018). According to the 4+4+4 method, it is assumed that 4 hours of a 12-hours daylight day are close to WBGTmax, other 4 hours (early morning and early evening) are close to WBGTmean, and the remaining 4 hours are an average value of WBGTmean and WBGTmax. In our analysis, we calculate the average daily impacts on worker productivity under WBGTmax, WBGTmean, and an average value of WBGTmean and WBGTmax.

2.3 Exposure-response functions

To calculate the productivity losses due to HS, we use the exposure-response function derived by Kjellstrom et al. (2018) and further used by Bröde et al. (2018) for the "high occupational temperature health and productivity suppression" programme (Hothaps) (hereafter: the Hothaps function). The calibration of the Hothaps function is based on empirical epidemiological studies conducted by Wyndham (1969) and Sahu et al. (2013). The Hothaps function is a two-parameter logistic function, which describes the relationship between worker productivity and WBGT for different levels of work intensity:

$$Workability = 0.1 + \frac{0.9}{\left(1+\left(\frac{WBGT}{\alpha_1}\right)^{\alpha_2}\right)} \quad \text{(Eq. 2.3.1)}$$

where α_1 and α_2 are the estimated parameters for low-intensity work (34.64 and 22.72), for moderate-intensity work (32.93 and 17.81), and for high-intensity work (30.94 and 16.64). Fig. 2 illustrate the relationship between worker productivity loss due to HS and WBGT, derived from the Hothaps function.

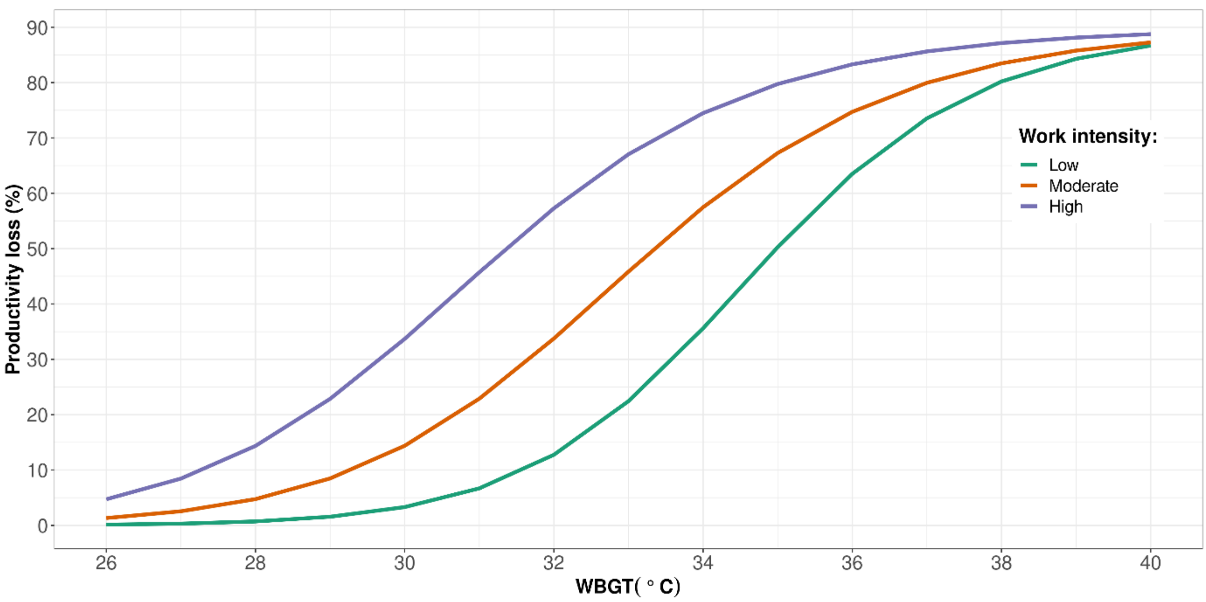

Fig. 2: Exposure-response functions based on the Hothaps metric. The impacts on productivity were measured at an hourly basis in the field studies on which the exposure-response function was calibrated. Bröde et al. (2018) assume that "working is possible for 6 min within each hour even under extreme heat". Therefore, productivity loss does not reach 100% even under high heat stress levels.

Work intensity is described by metabolic rates measured in Watts (W). According to Kjellstrom et al. (2009), an average metabolic rate for low-intensity work accounts for 200 W, for moderate-intensity work, it is 300 W, and for high-intensity work, it is 400 W. The service and manufacturing sectors require mainly indoor work, while agriculture and construction typically involve outdoor labour. Therefore, to calculate heat-induced impacts on worker productivity in agriculture and construction, we use the WBGTsun, whereas for services and manufacturing, the WBGTshade is implemented. As mentioned above, the value of WBGTsun is higher than that of WBGTshade since people working outdoors are exposed to an additional HS due to solar radiation. On the other hand, wind could alleviate the HS through a cooling effect. Following previous studies (Kjellstrom et al., 2018), agriculture and construction are assumed to be high-intensity jobs (400 W), while manufacturing and services require moderate-intensity (300 W) and low-intensity work (200 W), respectively.

Physical responses (i.e., relative worker productivity losses) are also calculated on a daily basis for each grid cell and for each level of work intensity. Then, the spatiotemporal data on heat-induced reductions in worker productivity is matched with the gridded data on the population count to obtain population-weighted impacts on worker productivity at a regional level. To weight the impacts for the historical reference period, we use the gridded UN WPP-adjusted population count data provided by CIESIN (2017), while the impacts under RCP2.6 and RCP8.5 are weighted by the spatial population projections associated with the shared socioeconomic pathways (SSPs) developed by Jones and O'Neill (2016) and further described in section 2.4. Finally, we calculate the deviations between the heat-induced reductions in worker productivity in the historical reference period and each RCP, respectively, so that we obtain the future impacts of HS on worker productivity resulting from global warming. These calculated physical impacts (i.e., relative reductions in work efficiency) are then implemented in the economic model described below.

2.4 Economic model

There are different approaches to assess economic costs arising from heat-induced reductions in worker productivity. For example, direct economic costs could be valuated using wage rates or value added. To assess aggregated impacts on GDP, one could use the so-called "first-order effects" approach; the sum of changes in worker productivity in production sectors, which are weighted by labour income shares in total GDP (Roson and Sartori, 2016). However, indirect effects related to the interdependencies between economic sectors are thereby ignored. In our analysis, we employ a recursive-dynamic multi-region, multi-sector computable general equilibrium (CGE) model, GRACE (Aaheim et al., 2018). CGE models are widely used for impact assessments and policy evaluations (Château et al., 2014; Corong et al., 2017). The framework of a CGE model enables to consistently depict sectoral and regional interdependencies, thereby providing a comprehensive valuation of socio-economic costs. The static version of GRACE is calibrated around Version 9 of the GTAP database (Angel et al., 2016), which depicts global economic transactions in 2011 for 140 regions and 57 sectors. All values in Version 9 of the GTAP database are expressed in US$2011. We aggregate all regions into 10 regions, which are Africa, East Asia, South Asia, South-East Asia, West Asia, Europe, North America, South America, Oceania, and Former Soviet Union (FSU) (see Fig. 3 and supplementary material, SM2). Note that several countries, in particular African countries, are missing in the used version of the GTAP database. Hence, aggregated impacts for the regions of Africa could be biased. All production sectors are aggregated into 12 sectors, which are crops, livestock, food, services, manufacturing, transport, construction, crude oil, oil refinery, coal, electricity, and gas (see supplementary material, SM2). To calibrate the dynamic version of GRACE from 2011 to 2100, we use the projections of gross domestic product (GDP) and population growth rates associated with SSPs (see supplementary material, SM3). SSPs describe different possible socio-economic pathways (i.e., economic development, population growth, land use, and energy consumption), which help to understand long-term consequences of near-term decisions (Riahi et al., 2017). The model was run under the pathways SSP1, SSP4 and SSP5. SSP5 ("Fossil-fueled Development") describes a world with high economic growth relying on fossil fuel consumption, high challenges to mitigation but low challenges to adaptation; SSP4 ("Inequality") implies high inequality among regions with low challenges to mitigation but high challenges to adaptation; and SSP1 ("Sustainability") is a world on a sustainable development pathway with low challenges to mitigation and adaptation (Riahi et al., 2017). While SSP5 is characterised by relatively high growth rates of GDP per capita, SSP1 and SSP4 are associated with a lower economic growth among regions. The growth rates of SSP1 and SSP4 are very similar for Oceania, North America, and Europe, whereas these significantly differ by developing countries with the economic growth being less pronounced under SSP4. This is because SSP4 is designed to depict a world with growing income inequality both across and within regions (Calvin et al., 2017). For more details on key differences among SSPs, we refer to Riahi et al. (2017).

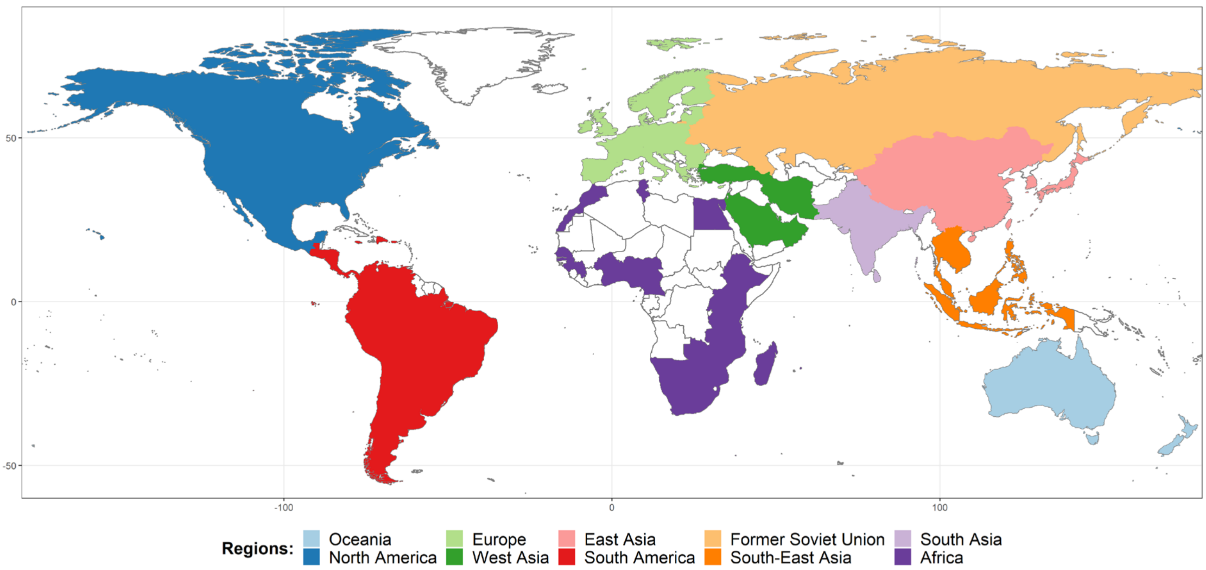

Fig. 3: Regional mapping.

The reference scenario in the GRACE model is calibrated given the assumption of a balance growth path, i.e., the ratio of capital and labour is held constant. A structural change is depicted by using a Stone-Geary utility function, which implies different income elasticities of demand for commodities and services. Income elasticities of demand for food products are empirically estimated using the FAO and World Bank databases (see supplementary material, SM4). Income elasticities of demand for other goods and services are derived from Chapter 14 of the GTAP database (Hertel and Mensbrugghe, 2016). Levels of subsistence consumption for each demand category are re-calibrated by population growth. Furthermore, following Britz and Roson (2019), we implement differentiated productivity growth for agriculture, manufacturing, and services (see supplementary material, SM5). Both differentiated income elasticities and sectoral productivity drive structural changes. We assume no labour mobility across borders (i.e., no migration), while labour and capital are mobile among sectors within a region. Moreover, capital is assumed to be mobile across regions. Trade elasticities are adopted from the GTAP model. Sectoral production is described by nested constant elasticity of substitution (CES) functions over intermediates, labour, capital, and natural resources. So, labour enters the production function as an input (i.e., primary production factor). In the model, heat-induced reductions in worker productivity are implemented through reductions in the parameters depicting labour efficiency in the CES aggregate. Consequently, changes in labour efficiency affect the sectorial output. For more details on the model structure and underlying assumptions, we refer to Aaheim et al. (2018).

2.5 Air conditioning

Air conditioning devices are an effective adaptation strategy to avoid or at least substantially reduce HS in the indoor environment. Using the logistic function estimated by Isaac and van Vuuren (2009) based on the data on the penetration of air conditioners (AC) in the residential sector in various countries collected by McNeil and Letschert (2008), we calibrate the penetration rates of AC for the aggregated regions of interest. Eq. 2.5.1 shows the relationship between the availability (or affordability) of AC and income measured as GDP per capita measured in U.S. dollars (2011).

$$Availability = \frac{1}{\left(1+e^{\left(4.152-0.237*\frac{Income}{1000}\right)}\right)} \quad \text{(Eq. 2.5.1)}$$

The calculated penetration rates of AC by region and SSP are illustrated in Fig. 4. A higher penetration rate of AC implies a lower exposure to HS in the indoor environment. We assume that when the penetration rate of AC reaches its maximum value (i.e., equal unity), the productivity of indoor work is not any longer affected by HS. By the middle of the century, the diffusion of AC in developed countries reaches its saturation. For developing countries, the installation of AC occurs rapidly under SSP5, followed by SSP1, while under SSP4, it proceeds very slow; for example, in many developing countries, the penetration rate is less than 50% even by 2100.

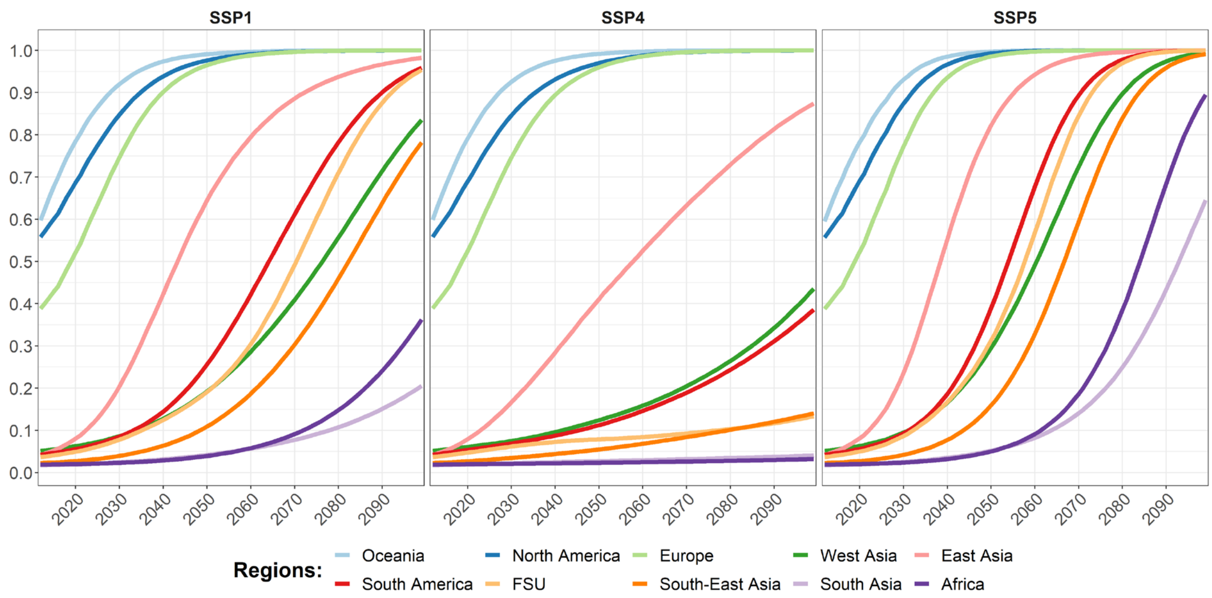

Fig. 4: Penetration rates of air conditioners by region and SSP.

Note that the calibrated logistic function developed by Isaac and van Vuuren (2009) describes the availability of AC in the residential sector only, but the penetration of AC in industries at workplace could differ. Due to a lack of data, we assume that the penetration of AC in the manufacturing and services sector follows the same trajectory.

2.6 Work intensity and economic growth

While installation of AC could effectively alleviate heat-induced reductions in worker productivity of indoor jobs, automation and mechanisation is likely to be one of most effective adaptation strategies for outdoor work, in particular if shifting working hours is problematic. In previous studies, it was assumed that agriculture and construction require high-intensity jobs with a metabolic rate of 400 W for all regions. However, work intensity of outdoor jobs likely differs by country due to differences in economic development. A plausible assumption is that, due to a higher level of mechanisation, agricultural and construction sectors in developed countries are less work intensive (or more capital-intensive) compared to those in developing countries. Moreover, economic development will lead to a further increase in mechanisation of work in both developed and developing countries, which in turn will alleviate adverse heat-induced impacts on worker productivity. Thus, assuming the same constant work intensity for all countries could lead to biased results.

In the Hothaps function, the vulnerability to HS is captured by two parameters (i.e., α_1 and α_2), which are calibrated for only three types of work intensity (see Eq. 3.3.1). We use a linear interpolation to synthesise those parameters for different levels of work intensity, so the parameters α_1 and α_2 become a function of work intensity. The number of tractors per 100 km^2 of arable land, which is available at the World Bank database (World Bank, 2019), serves as an indicator of mechanisation and work intensity in agriculture. We empirically estimate the relationship between economic growth and the availability of tractors among countries (see supplementary material, SM6). These estimates are then used to map different levels of work intensity with the economic growth. Based on existing studies assessing energy costs for different types of jobs (Poulianiti et al., 2019), we find that the metabolic energy use associated with manual work in agriculture is 1.5 times as high as in mechanised work. So, we assumed that agriculture in countries with the lowest number of tractors has work intensity of 400 W, whereas in countries with the highest mechanisation, it equals 267 W (see supplementary material, SM6). Because data on machinery and equipment used in construction are not available, we assume that the relationship between economic growth and work intensity in construction is the same as in agriculture. Finally, we obtain new exposure-response functions, whose parametrisation depends on the economic growth (see Fig. 4). For example, the calibrated work intensity of agriculture and construction in developed countries in 2011 is around 370 W, while in developing countries, it is close to 400 W. Economic growth, which is depicted by SSPs, leads to a lower work intensity due to mechanisation. Under SSP5, reductions in work intensity are substantial in all regions, whereas under SSP1 and SSP4, these are less pronounced. In particular for developing countries, reductions in work intensity are moderate under SSP4, as illustrated by relatively flat curves in Fig. 5 (i.e., SSP4 implies the lowest adaptation capacity). Mechanisation of outdoor work is autonomously implemented in the model for each scenario, and it depends solely on the assumed economic growth. In other words, mechanisation is exogenously determined, and it does not change in response to increased heat levels.

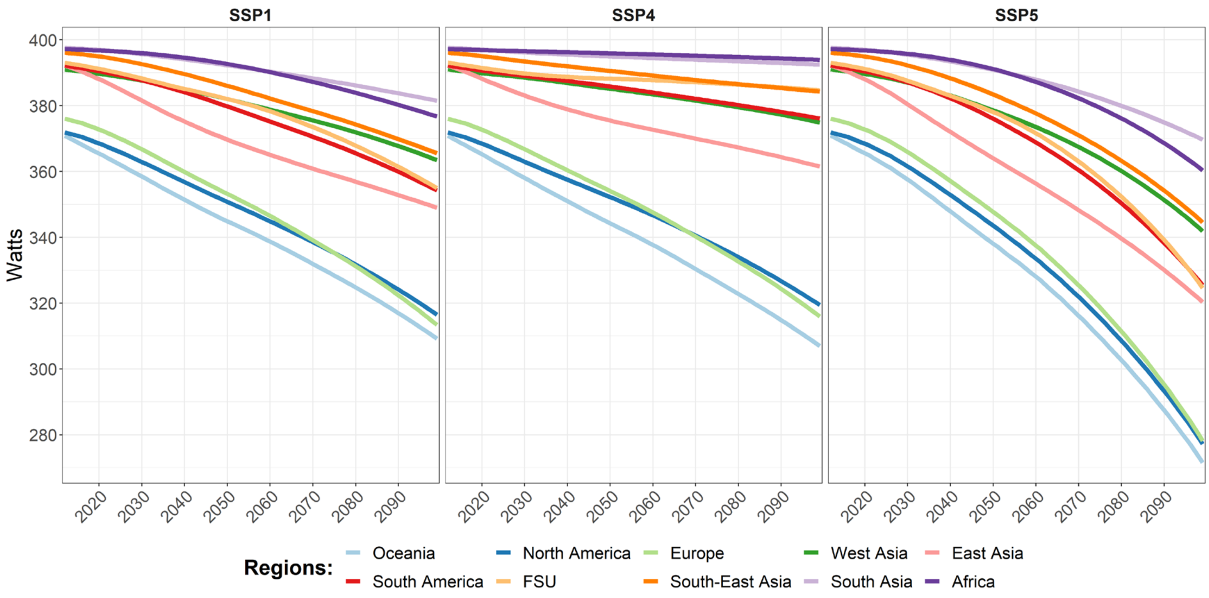

Fig. 5: Calibrated relationship between economic growth and work intensity in agriculture and construction.

2.7 Scenarios and uncertainties

Here we summarise our scenario setting. We consider three main scenarios, RCP8.5-SSP5, RCP2.6-SSP1, and RCP2.6-SSP4, which are conducted under different modelling assumptions and parameterisation. Model results are presented in relative terms and should be interpreted as changes relative to the reference scenario with no climate change (NoCC). In our analysis, we address several types of uncertainties:

- **Climate models.** This analysis is based on climate data from two climate models, GFDL-ESM2M and HadGEM2-ES, which allows us to capture uncertainties related to the choice of underlying GCMs.
- **Socio-economic pathways.** SSPs provide projections of economic and population growth. RCP8.5 is combined with SSP5 only, whereas several SSPs are plausible in combination with RCP2.6. To tackle socio-economic uncertainties, we map RCP2.6 with SSP1 and SSP4, where the former aims to depict a sustainable pathway with low challenges to mitigation and adaption, and the latter describes a world with increasing income inequality within and across countries and low challenges to mitigation but high challenges to adaptation. Note that SSPs were constructed by different institutes such as IIASA, OECD, and PIK, which made different assumptions about future economic and population growth. We take mean values of those projections (i.e., GDP and population growth) to represent the individual SSPs.
- **Sectoral labour mobility.** In the core version of the GRACE model, labour is assumed to be perfectly mobile across sectors. To investigate the sensitivity of model results with respect to the assumption of sectoral labour mobility, following Dixon and Rimmer (2006), we implement inertia in the labour market by using a constant elasticity of transformation (CET) function with a transformation elasticity of 2.
- **Capital-labour substitution.** To test the robustness of model results with respect to the value of substitution elasticities between capital and labour, we conduct a sensitivity analysis using a plausible range of substitution elasticities of 0.3–0.7. The core value of the substitution elasticity within the value-added aggregate equals 0.5.

Results from a CGE model are typically sensitive to the parameterisation of the model where a shock is implemented. Regarding this case study, a shock is implemented on labour productivity, so the parametrisation of the labour market could be important (e.g., substitution elasticities within the value added and labour mobility). Other factors such as trade elasticities might also be relevant. Yet, we tested the robustness of model results with respect to different values of trade elasticities among regions; the sensitivity analysis showed that results remain robust.

3. Results and discussion

3.1 Macroeconomic impacts

The model results show that HS leads to substantial reductions in worker productivity, especially the productivity of high intensity work in low-latitude countries of Africa, South America, and Asia. Given the assumption of absence of AC and constant work intensity, reductions in worker productivity in some regions under RCP8.5 could even exceed 40% by 2100 compared to NoCC (see Fig. 6a, b).

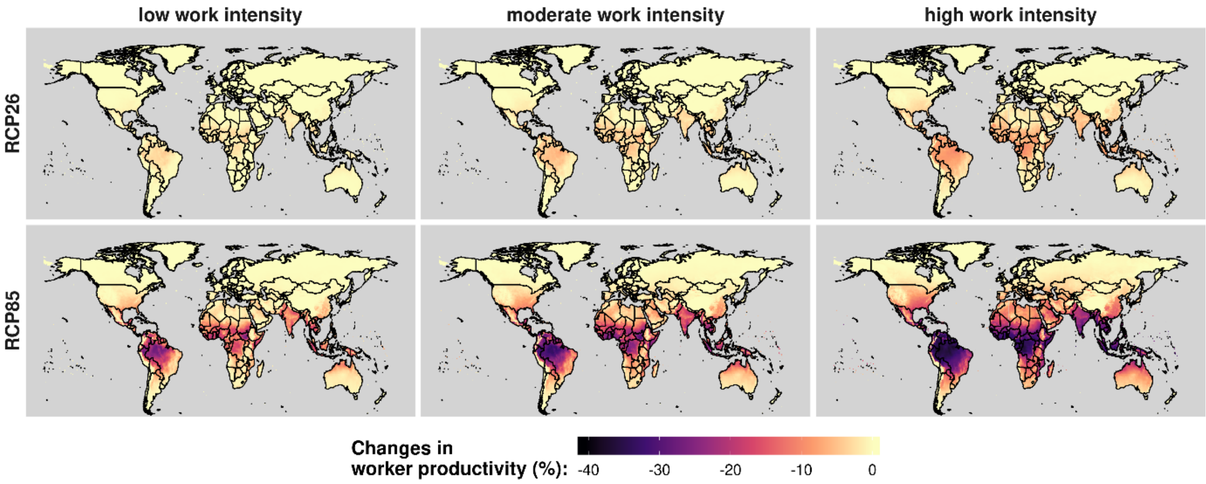

Fig. 6a: Average changes in worker productivity for levels of different work intensity and RCP scenarios by 2100 relative to the reference scenario with no climate change. The Hothaps function is used to estimate the heat impacts on worker productivity. Adaptation measures, such as air conditioners and mechanisation of work, are not implemented at grid cell levels. Low and moderate work intensity implies work indoors (i.e., services and manufacturing), while a high work intensity implies work outdoors (i.e., agriculture and construction).

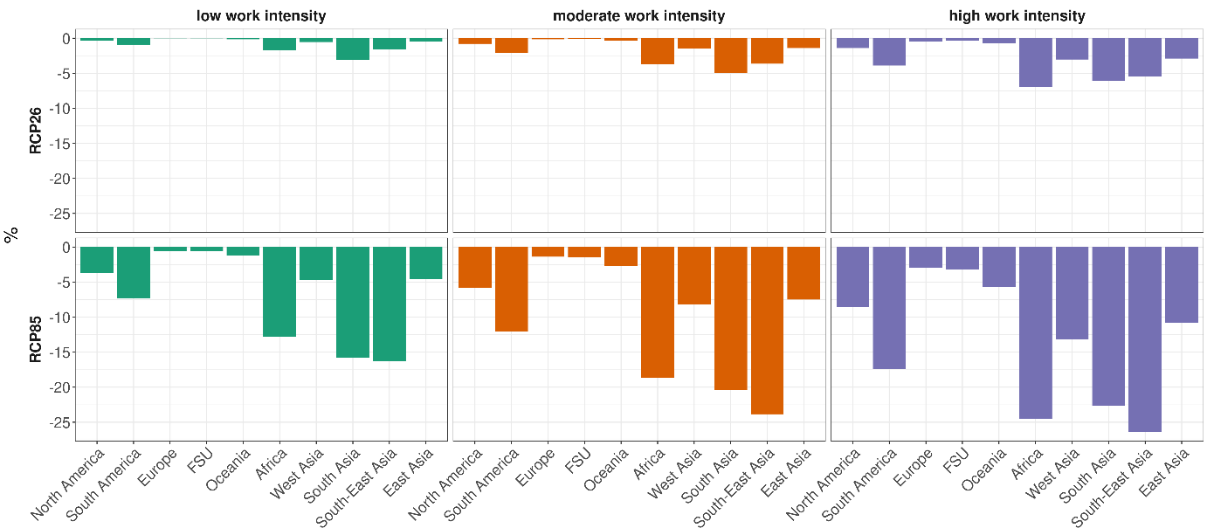

Fig. 6b: Same as Fig. 6a but showing the regional aggregated population-weighted average changes in worker productivity.

3.1.1 Global economic impacts

Hothaps vs. ISO

In contrast to previous economic studies, which used occupational health and safety recommendations (e.g., ISO 7243:1989) (ISO, 1989) as a heat stress assessment metric, we use the epidemiological exposure-response (Hothaps) function calibrated based on field studies. We find that when using the Hothaps function, reductions in global GDP are considerably less pronounced than under the ISO 7243:1989 standards. For example, under RCP2.6 by 2050 and 2100, the average reduction in global GDP is around 0.5% relative to NoCC, which is approximately 0.4 percentage points lower than when the ISO 7243:1989 standards are used. For RCP8.5, using the Hothaps function with constant work intensity results in an average reduction of 0.7% (1.8%) in global GDP by 2050 (2100) relative to NoCC, which is 0.6 percentage points lower than when the ISO 7243:1989 standards are used. Comparing to previous studies, Takakura et al. (2017) find that under the highest emission scenario, the average cost of preventing heat-related illness accounts for 3.3% relative to NoCC. The ISO metric is more restrictive regarding work capacity during hot temperatures because it provides recommendations to avoid any heat related illness. Yet, not following the ISO standards at workplaces can increase the risk of heat related illness, which could imply additional economic costs of human health care and treatment. However, this type of costs is not accounted for in our analysis. The usage of the ISO metric for impact assessments maybe more relevant for well-regulated settings (i.e., developed countries), while the exposure-response function maybe more suitable for informal, unregulated settings (i.e., developing or least developed countries).

Mechanisation

Furthermore, assuming mechanisation of outdoor work, which implies decreasing work intensity, diminishes economic costs resulting from HS. Under RCP2.6, decreasing work intensity due to mechanisation does not have a strong impact on the results compared to the case when a constant work intensity is assumed. However, under RCP8.5 by 2100, reductions in global GDP are significantly lower when mechanisation is assumed (see the solid and dashed lines in Fig. 7). According to the model results, mechanisation in agriculture and construction diminishes the reduction in global GDP by approximately 0.4 percentage points. Note that the projected mechanisation of outdoor jobs is uncertain as it is based on a simple linear interpolation. On the one hand, a rapid technological change (i.e., robotisation) could lead to larger reductions in work intensity. However, a rapid diffusion of less labour-intensive technologies in poor countries could be seriously hindered by low income (i.e., a low affordability of new technologies). Therefore, we consider our estimates to be rather conservative.

Private consumption and mitigation costs

The estimated high economic costs induced by HS imply that large cost-savings could be achieved if the transition to a low-emission pathway of 2°C global warming target succeeds. According to the IPCC's Fifth Assessment Report (AR5), by 2100, the mean value of global mitigation costs of achieving a 2°C global warming target accounts for 4.8% of a reduction in global consumption relative to the baseline that implies no mitigation policies (i.e., RCP8.5) (IPCC, 2014). The results from our model simulations reveal that when using the Hothaps function and assuming autonomous mechanisation, global private consumption falls by 2% under RCP8.5 by 2100 (see supplementary material, SM7). This implies that approximately 42% of the global mitigation cost could be offset by avoiding the adverse impacts of HS on worker productivity. However, not all regions would benefit equally from that; in some high-latitude countries, which are less exposed and vulnerable to heat stress, mitigation costs could exceed the benefit of avoiding climate-induced warming.

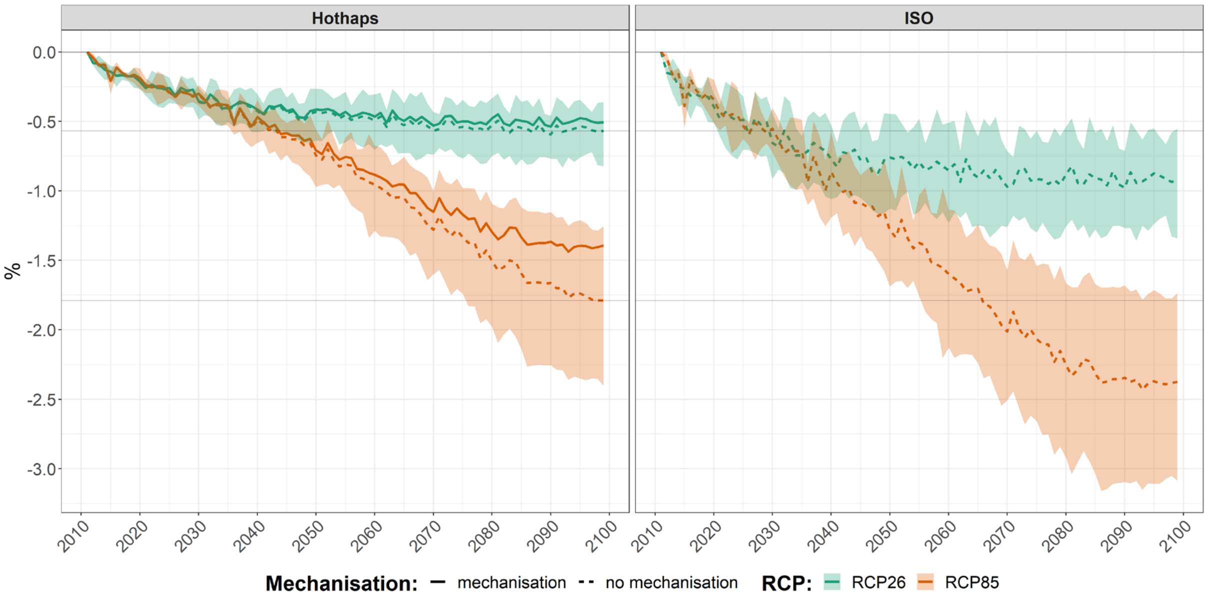

Fig. 7: Changes in global GDP under RCP2.6 and RCP8.5 compared to the reference scenario with no climate change. The solid and dashed lines show the mean values and the shaded areas indicate uncertainties in the estimated impacts. In the plot legend, "mechanisation" (solid lines) stands for decreasing work intensity due to mechanisation driven by an economic growth, while "no mechanisation" (dashed lines) implies a constant work intensity. "Hothaps" stands for the epidemiological exposure-response function, while "ISO" implies that ISO: 7243:1989 standards are used to assess heat stress impacts on worker productivity.

3.1.2 Uncertainties

As illustrated by shaded areas in Figure 7, economic costs of HS are very uncertain; for example, when using the Hothaps function, the reduction in global GDP could reach 2.4% under RCP8.5 by 2100. The results from an ANOVA analysis reveal that until the middle of the century, the largest fraction of the variance (62%) in the results is explained by uncertainties around GCMs, followed by the uncertainty of mitigation scenarios (i.e., RCP2.6 vs. RCP8.5), which explains around 33% of the variance (see Fig. SM7.2 in supplementary material). In the second half of the century, the uncertainty of mitigation scenarios becomes more relevant; for example, by 2100, approximately 73% of the variance in the results is explained by differences between RCP2.6 and RCP8.5, whereas using different climate models explains 22% of the variance. Using the output from the GFDL-EMSM2M model leads to much less pronounced reductions in global GDP compared to HadGEM2-ES (see Fig. SM7.3 in supplementary material). This could be explained by different assumptions about climate sensitivity between these two GCMs. Interestingly, the results are less sensitive to the socio-economic uncertainties, such as sectoral labour mobility, economic and population growth (i.e., SSPs), and substitution elasticities in production. Although overall socio-economic conditions are certainly important, the uncertainty of climate modelling and mitigation scenarios drive a larger variance in the results. In our analysis, we consider a combination of RCP2.6 with SSP1 and SSP4, whereas RCP8.5 is combined only with SSP5. The differences in the estimated economic costs under RCP2.6-SSP1 and RCP2.6-SSP4 are moderate because the impacts of HS under RCP2.6 are relatively small.

3.1.3 Regional economic impacts

Economic costs resulting from heat-induced reductions in worker productivity vary substantially across geographical regions. Under RCP2.6 by 2050, changes in real GDP in rich regions, such as Europe, North America, and Oceania, are negligible, whereas Africa, South-East Asia (e.g., Indonesia, Thailand, and Vietnam) and South Asia (e.g., India, Pakistan, and Bangladesh) experience considerable economic losses, i.e., reductions in real GDP are larger than 1% (see Fig. 8). Overall, under RCP2.6 by 2100, the impacts on regional GDPs are of the same order of magnitude as compared to 2050 since radiative forcing stabilises by the middle of the century under this scenario. High economic costs in African and Asian countries are explained by i) a strong increase in temperatures, ii) a low capacity to adapt, and iii) the composition of employment. In developing countries, the share of agriculture in GDP and the share of workers employed in agriculture, which are at a high risk of suffering HS impacts, is considerably larger than in developed countries. Furthermore, many countries that are the most affected by HS have high working poverty rates, informal employment, subsistence agriculture, and a lower social security coverage (Kjellstrom et al., 2019).

Under RCP8.5, the pattern of reductions in regional GDPs is very similar to that of RCP2.6, but the quantitative impacts are of larger magnitude compared to RCP2.6 due to higher temperatures and non-linearities in the exposure-response relationship. For example, under RCP8.5 by 2050 (2100), an average reduction in real GDP of Africa accounts for 2.7% (3.6%), for South-East Asia, it is 3.5% (2.4%), and for South Asia, it is 4.2% (6%). There are uncertainties in the estimated impacts; for example, the reduction in GDP of South Asia could reach 8%. Overall, an average reduction in real GDP across regions under RCP8.5 by 2050 (2100) is 1.9 (2.6) times as large as under RCP2.6. The combination of RCP8.5-SSP5 implies a higher economic growth and therefore, a higher adaptative capacity compared to RCP2.6-SSP1/SSP4. Nevertheless, adverse heat-induced impacts on worker productivity under RCP8.5 are substantially greater than under a 2°C pathway, so the adverse impacts of HS outweigh the effect of having a higher adaptative capacity. Note that the reported relative changes in regional GDPs could substantially differ within a region as well as among different household groups. The impacts on total private consumption by region, which are often considered as an alternative measure of welfare to GDP, can be found in supplementary material (see Figure SM7.4). Reductions in total private consumption have a similar pattern but more pronounced compared to the impacts on GDP. The results from model simulations also show that changes in private consumption are very similar to changes in real disposable income. While private consumption implies expenditures on consumption of goods and services, disposable income also include savings.

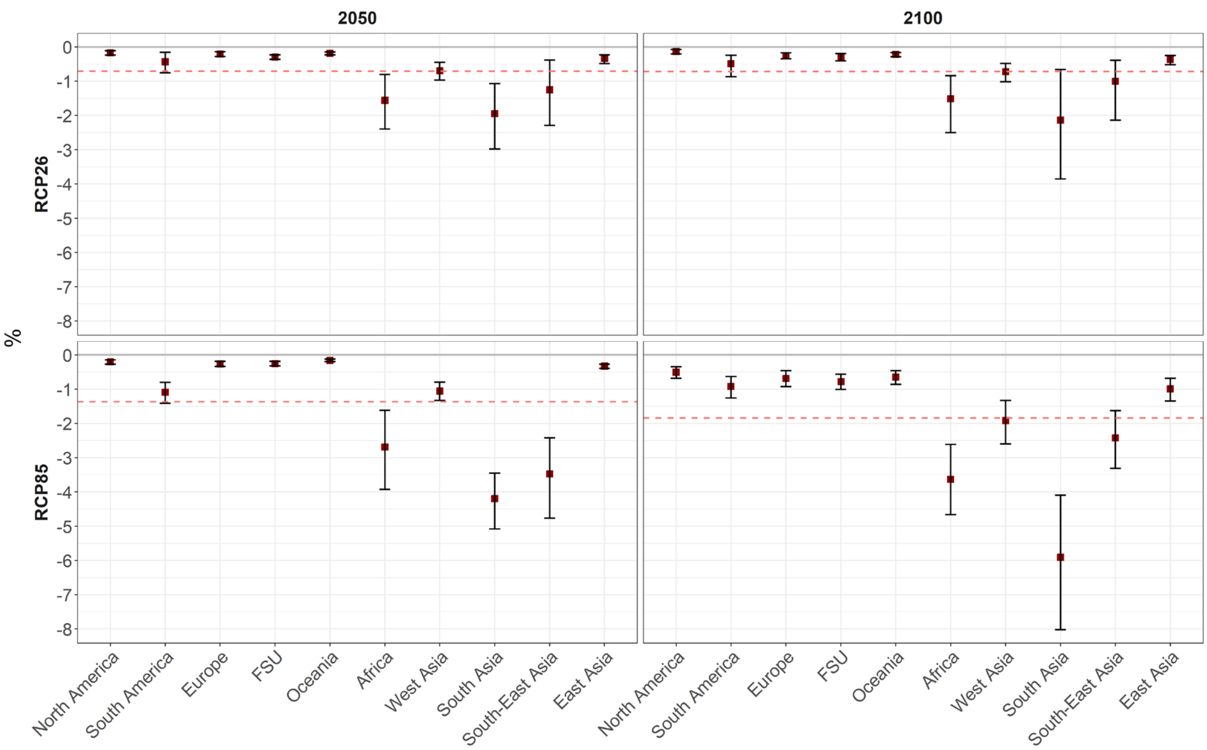

Fig. 8: Changes in regional GDP under RCP2.6 and RCP8.5 by 2050 and 2100 compared to the reference scenario with no climate change. The Hothaps function is used to estimate the heat impacts on worker productivity. Dashed read line shows the mean values across regions, and the error bars indicate the uncertainties in the estimates.

3.2 Sectoral impacts

3.2.1 Agriculture and construction

Agriculture (i.e., crops and livestock) and construction are the most adversely affected by HS because these sectors require many work-intensive activities in the outdoor environment. Even under RCP2.6 some regions, such as Africa and Asia, experience substantial reductions in worker productivity in these sectors, while under RCP8.5, the reductions are significantly larger (Fig. 9). For example, under RCP8.5 by 2050, an average reduction in worker productivity in agriculture and construction across regions accounts for almost 4.2% relative to NoCC, whereas for South-East Asia, it is approximately 11%. Decreasing worker productivity due to HS affects the production output, but this relationship is not one-to-one because of demand responses. So, relative reductions of production in agriculture and construction are lower than the impacts on worker productivity; an average reduction in production of crops across regions under RCP8.5 by 2050 amounts to 0.8% relative to NoCC, for livestock, it is 1.3%, and for construction, it is 2.1%. Furthermore, there are even slight increases in production of agricultural goods in Oceania, North America, FSU, and Europe. Intuitively, demand for agricultural goods tends to be inelastic, i.e., a reduction in supplies is associated with a relatively larger increase in prices. According to the model results, a decreased worker productivity in agriculture leads to a lower production, thereby resulting in higher prices. Therefore, for producers, economic costs from heat-induced reductions in worker productivity are in part compensated by increased food prices. In the applied economic model, GRACE, there are also cross-regional interactions occurring through trade. While many low-latitude regions experience considerable reductions in worker productivity, less vulnerable regions to HS, such as Oceania, North America, FSU, and Europe, receive a comparative advantage in production of agricultural goods, which explains those moderate increases in their production. As a result, exports of crops from those regions increase (Fig. 10). It is worth noting that the developed countries have relatively lower employment rates in agriculture compared to developing countries, and therefore, developed economies are less vulnerable to HS impacts in agriculture.

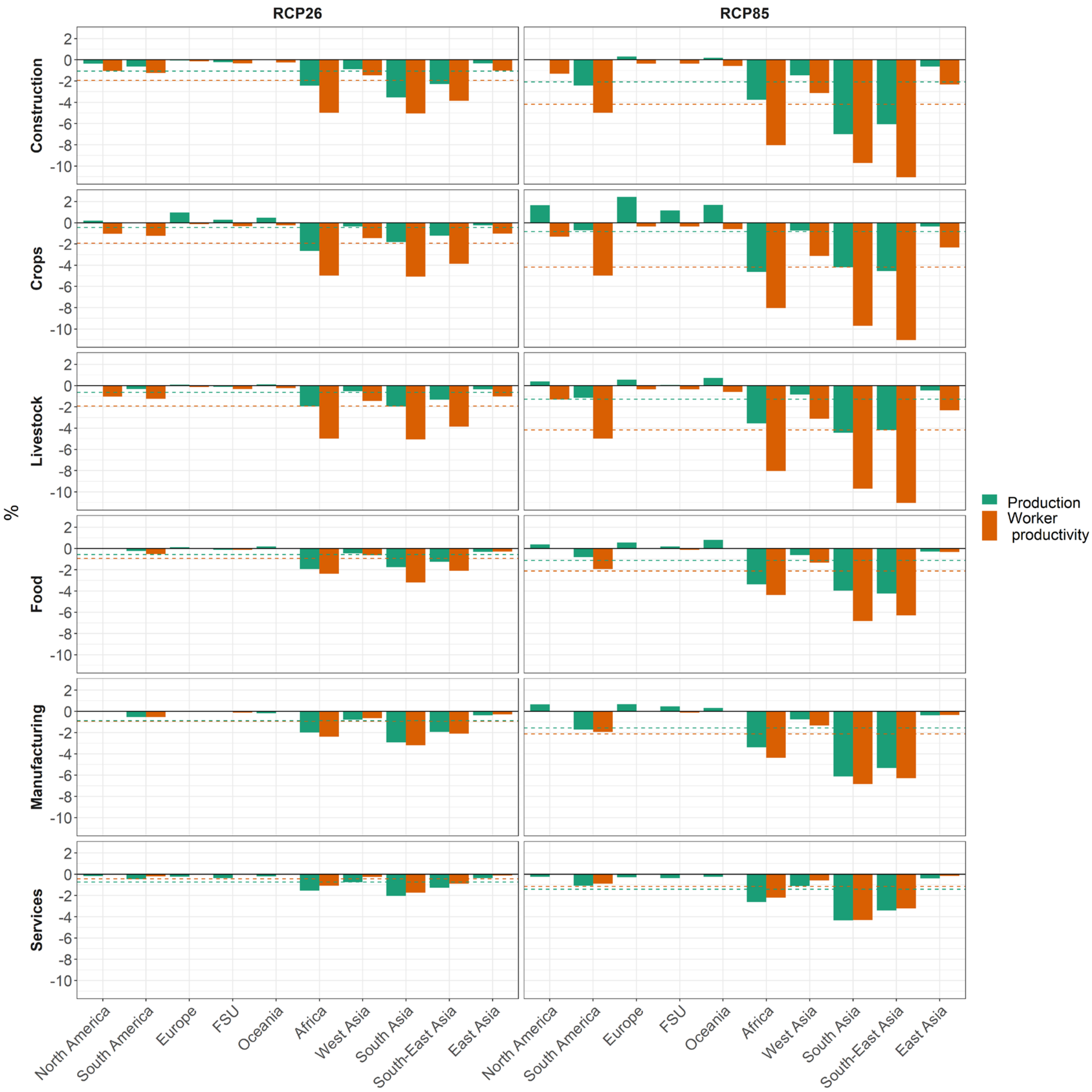

Fig. 9: Average heat-induced changes in worker productivity and production by 2050 under RCP2.6 and RCP8.5 relative to the reference scenario with no climate change. The Hothaps function is used to estimate the heat impacts on worker productivity. The dashed lines show the mean values across regions.

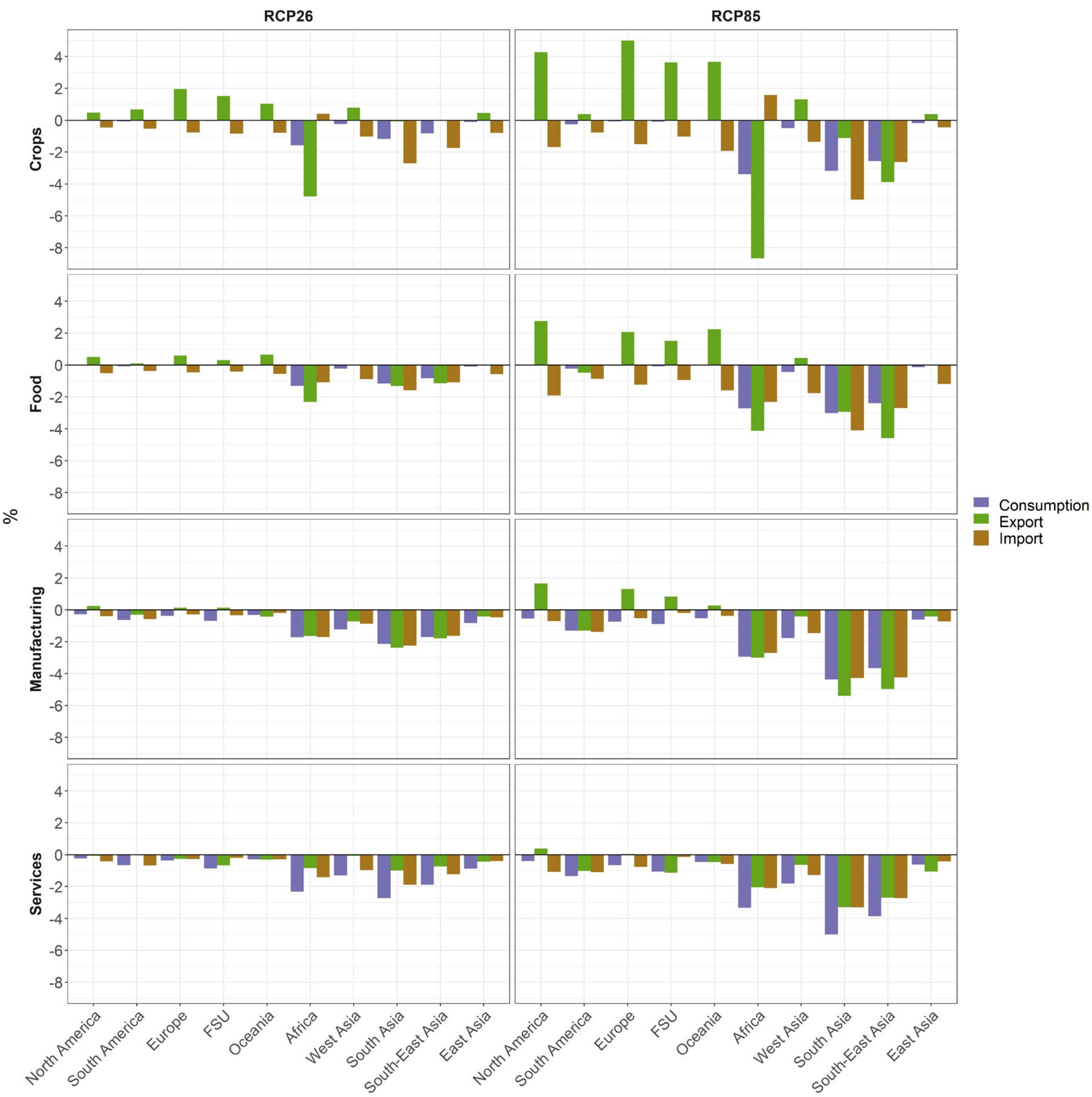

Fig. 10: Average heat-induced changes in private consumption, exports, and imports by 2050 under RCP2.6 and RCP8.5 relative to the reference scenario with no climate change. The Hothaps function is used to estimate the heat impacts on worker productivity. The impacts on construction and livestock are not shown here because these are non-tradable goods and services.

Given the assumption that a large share of low-income population is employed in agriculture and construction as low-skilled workers, HS could also, to some extent, exacerbate income inequality in those regions. Note that our analysis focuses entirely on heat impacts on worker productivity, but droughts (often co-occurring with heatwaves) could also reduce crop yields, thereby decreasing economic output of farmers in heat-exposed regions.

3.2.2 Manufacturing

Due to the penetration of AC and a lower work intensity, manufacturing is less adversely affected by HS compared to agriculture and construction. Because of solar radiation, heat-induced impacts on worker productivity in agriculture and construction are stronger than in manufacturing and services, where work is mainly undertaken indoors. This also explains why the production of manufactured goods including food is less exposed to HS compared to agriculture and construction (Fig. 9). Under RCP8.5 by 2050, the worker productivity and production of manufactured goods across regions decline by an average of 2.1% and 1.6% relative to NoCC, respectively. For RCP2.6, an average reduction in both worker productivity and production across regions accounts for approximately 1%. Differences between relative reductions in worker productivity and production of manufactured goods are less pronounced compared to those in agriculture and construction. This is mainly because the demand for many types of manufactured goods is more elastic than for agricultural goods, so the price effect tends to be smaller. While developed regions (i.e., Europe, North America and Oceania) experience slight increases in the production of manufactured goods, many African, South-East Asian, and South Asian countries have considerable reductions in the production. For example, under RCP8.5 by 2050, production of manufactured goods in South Asia falls by an average of 6.1%. In contrast, production and export supplies of manufactured goods from North America, Europe, and FSU increase (Fig. 9 and 10). Also, there are increases in the exports of food products from those regions. Private consumption and imports of manufactured goods fall across regions, especially those most adversely affected by HS.

3.2.3 Services

The service sector exhibits a low risk of exposure to HS, because of penetration of AC and the lowest work intensity among production sectors. Moreover, like the production of manufactured goods, the service sector requires mainly indoor jobs. However, relative reductions in production of services are larger than actual impacts of HS on worker productivity because of decreased income. Under RCP2.6 (RCP8.5) by 2050, an average reduction in the production of services across regions is 0.7% (1.4%) relative to NoCC, whereas for South Asia, it is 2% (4.3%). Like manufacturing, private consumption and imports of services decline across regions, especially in Africa and Asia. Nowadays, the penetration rate of AC is relatively high in developed countries, and it is expected to further increase because of economic growth, thereby completely offsetting moderate impacts of increased temperatures in those countries. For developing countries, where AC are not yet widely installed in the commercial and residential sectors, air conditioning also implies an effective adaptation measure to alleviate heat-related human health risks and to avoid reductions in worker productivity. Yet, this type of adaptive capacity is virtually limited by affordability of AC (i.e., households' income); a low income could prevent a rapid installation of AC.

Due to large uncertainties of future mitigation pathways, sectoral impacts by 2100 are of less interest. Nevertheless, we briefly highlight some main findings. Under RCP2.6, the heat-induced impacts on the production of goods and services by 2100 do not differ much from those by 2050 because according to a 2°C pathway, radiative forcing should stabilise after the middle of the century. In contrast, under RCP8.5, adverse sectoral impacts, especially in developing regions, become more pronounced by 2100 compared to 2050 (see Figure SM7.5 in supplementary material). Note that this analysis was conducted at a very aggregated sectoral level; the impacts of HS could significantly differ within a sector because of differences in work intensity and heat exposure.

3.3 Limitations

Several limitations to our analysis should be noted. First, our study does not provide a comprehensive assessment of heat impacts because extreme heat could induce several other impacts on economies and society (e.g., impacts on mortality, morbidity, crop yields, and demand and supply of energy), which could also lead to substantial socio-economic losses. Our analysis is based on a CGE model, which is widely used for economic impact assessments; however, CGE models are typically not empirically validated. There are big uncertainties on how to properly depict demand and supply responses as well as trade in large-scale CGE models. Furthermore, the epidemiological exposure-response function applied in this study is calibrated based on a limited number of field studies only. The estimated relationship between heat levels and worker productivity could differ among regions. More empirical research on exposure-response relationship is strongly needed. We implement an autonomous penetration of AC and mechanisation of outdoor work. While the role of mitigation policies is crucial for reducing HS impacts, a proactive promotion of those adaptation measures could diminish economic costs from HS. Nevertheless, it requires additional investments for purchasing new technologies and increases expenditures on electricity (i.e., air conditioning). It is worth mentioning that increased usage of air conditioners could potentially lead to higher CO_2 emissions, depending on the share of fossil fuel based power generation (Akpinar-Ferrand and Singh, 2010). Modelling an endogenous diffusion of labour-saving technologies and penetration of AC is a potential subject for future research. Some other adaptation measures to rising temperatures, such as shifting working hours and wearing cooling vests, are not implemented in this analysis. The urban heat island effect was also not considered. WBGT was calculated using daily levels of climate variables, while more accurate estimates of heat exposure require hourly data, though it is not obvious whether a finer temporal resolution would significantly change the macro-economic results. Heat acclimatisation, which could also reduce vulnerability to heat, was not considered in this study.

4. Conclusions

Using an interdisciplinary approach, which combines climate projections, epidemiological and economic analyses, we assessed the economic cost of heat-induced reductions in worker productivity under RCP2.6 and RCP8.5 and different socio-economic assumptions. We use historical and future climate projections from the ISIMIP. For our economic impact assessment, we use an empirically estimated epidemiological exposure-response (Hothaps) function and a dynamic multi-region, multi-sector CGE model. We find that when using the Hothaps function as a heat assessment metric and assuming autonomous mechanisation for outdoor work in agriculture and construction, average economic costs due to heat stress under RCP8.5 by 2100 account for a 1.4% reduction in global GDP relative to the reference scenario with no climate change. Autonomous mechanisation diminishes the reduction in global GDP by approximately 0.4 percentage points. For comparison, when occupational health and safety recommendations, such as the ISO 7243:1989 standards, are used for the economic impact assessment, global GDP falls by an average of 2.4%. Low-latitude countries of Africa, South-East Asia and South Asia are at a high risk of exposure to heat stress. Yet, strict mitigation policies aiming to achieve a 2°C global warming target substantially alleviate global economic costs from heat-induced reductions in worker productivity. For example, under RCP2.6, heat stress leads to an average decline of only 0.5% in global GDP by 2100. This implies that a large portion of mitigation costs could be offset by the benefit of reducing adverse heat-induced impacts on worker productivity. For example, according to the IPCC's Fifth Assessment Report (AR5), the mean value of global mitigation costs to reach a 2°C target is a 4.8% reduction in global private consumption relative to the reference scenario with no mitigation policy and no climate impacts. Our results show that, when economic costs are measured using the Hothaps function, global warming leads to an average reduction of 2% in global private consumption. This means that approximately 42% of the mitigation cost could be offset by avoiding the heat-induced reductions in worker productivity.

Acknowledgement

This work was funded by the Research Council of Norway and co-funded by the European Union through the project *"Tailored Climate Information for Investment Decisions"* (ClimINVEST) (grant agreement number 690462), which is part of ERA4CS, an ERA-NET initiated by JPI Climate. Also, this work was funded through the project *"Exposure to heat and air pollution in Europe – cardiopulmonary impacts and benefits of mitigation and adaptation"* (EXHAUSTION) that has received funding from Europeans Union's Horizon 2020 research and innovation programme under the grant agreement number 820655. The authors thank Nathalie Schaller for valuable improvement suggestions on the visualisation of results. Also, we would like to thank two anonymous referees for their very helpful comments and suggestions, which substantially improved the paper. The views and opinions expressed in this article are those of the authors and do not necessarily reflect the views of the Center for International Climate Research (CICERO).

Supplementary material

SM1: Calculation of WBGTsun

To approximate the Liljegren formula, we conduct a regression analysis on a chunk of climate data. Specifically, we calculated the WBGTsun using the Liljegren formula using daily data on air temperatures, dewpoint temperatures, solar radiation, and wind speed over the period of 2011-2020 from the GFDL-ESM2M model. The calculated WBGTsun enters the regression model as the response variable, while the explanatory variables are air temperatures, dewpoint temperatures, solar radiation, wind speed, latitude, and corresponding month. We test different linear and non-linear functions forms for the regression model, and we also run a support vector machine (SVM). We find that the SVM with a radial kernel provides a good approximation. But, using a 2nd order polynomial regression slightly outperforms the SVM and other functional forms in OLS in terms of accuracy, which is indicated by a high value of R^2 (see Table SM1). It should also be noted that estimating polynomial regression is much faster than SVM. Finally, the estimated coefficients from the 2nd order polynomial regression are used to calculate the WBGTsun for entire datasets.

This approximation approach has some limitations, however. The sun varies by hour, so does the heat stress. The Liljegren approach captures the sun component through the azimuth of the sun. For our analysis, we use the ISIMIP data, which provides only daily levels. To estimate the WBGTsun using the Liljegren approach, 12 UTC is used for zenith angle calculations. A more accurate estimation of WBGTsun would require hourly data. So, "hour" would be added as an additional explanatory variable into the regression model. Ideally, we should also validate this approximation method against observed WBGTsun. However, to our knowledge, there are a limited number of observations on WBGT. We consider the Liljegren approach as a benchmark, which produces the most accurate estimates for WBGTsun.

Table SM1.1: Regression results. Note: ‘Tas’ stands for air temperatures, ‘dp’ is dewpoint temperatures, ‘rsds’ is solar radiation, ‘sfcWind’ is wind speed, and ‘lat’ is latitude. Standard errors are in parentheses.

	2^{nd} order polynomial
(Intercept)	5.505349^{***}
	(0.001510)
Tas	0.414093^{***}
	(0.000101)
Tas^2	0.001620^{***}
	(0.000002)
dp	0.185106^{***}
	(0.000006)
dp^2	0.006278^{***}
	(0.000000)
rsds	0.005563^{***}
	(0.000002)
$rsds^2$	-0.000004^{***}
	(0.000000)
sfcWind	-0.344250^{***}
	(0.000040)
$sfcWind^2$	0.024530^{***}
	(0.000005)
Month	-0.004336^{***}
	(0.000025)
$Month^2$	0.000329^{***}
	(0.000002)
lat	0.000172^{***}
	(0.000001)
lat^2	-0.000007^{***}
	(0.000000)
R^2	0.998313
Adj. R^2	0.998313
Num. obs.	46590337
RMSE	0.126821

$^{***}p < 0.001$, $^{**}p < 0.01$, $^{*}p < 0.05$

SM2: Regional and sectoral mapping

Table SM2.1: Regional aggregation.

Regions	Countries
Africa	Egypt, Morocco, Tunisia, Rest of North Africa, Cameroon, Côte d'Ivoire, Ghana, Nigeria, Senegal, Rest of Western Africa, Rest of Central Africa, South Central Africa, Ethiopia, Kenya, Madagascar, Malawi, Mauritius, Mozambique, Tanzania, Uganda, Zambia, Zimbabwe, Rest of Eastern Africa, Botswana, Namibia, South Africa, Rest of South African Customs Union, Benin, Burkina Faso, Guinea, Togo, Rwanda
East Asia	China, Hong Kong SAR China, Japan, South Korea, Mongolia, Taiwan, Rest of East Asia
Europe	Austria, Belgium, Cyprus, Czechia, Denmark, Estonia, Finland, France, Germany, Greece, Hungary, Ireland, Italy, Latvia, Lithuania, Luxembourg, Malta, Netherlands, Poland, Portugal, Slovakia, Slovenia, Spain, Sweden, United Kingdom, Switzerland, Norway, Rest of European Free Trade Association, Albania, Bulgaria, Croatia, Romania, Rest of Eastern Europe, Rest of Europe
Former Soviet Union (FSU)	Belarus, Russia, Ukraine, Kazakhstan, Kyrgyzstan, Rest of Former Soviet Union, Armenia, Azerbaijan, Georgia, Rest of the World
North America	Canada, United States, Mexico, Rest of North America
Oceania	Australia, New Zealand, Rest of Oceania
South-East Asia	Cambodia, Indonesia, Laos, Malaysia, Philippines, Singapore, Thailand, Vietnam, Rest of Southeast Asia, Brunei
South America	Argentina, Bolivia, Brazil, Chile, Colombia, Ecuador, Paraguay, Peru, Uruguay, Venezuela, Rest of South America, Costa Rica, Guatemala, Honduras, Nicaragua, Panama, El Salvador, Rest of Central America, Rest of Caribbean, Dominican Republic, Jamaica, Trinidad & Tobago, Puerto Rico
South Asia	Bangladesh, India, Nepal, Pakistan, Sri Lanka, Rest of South Asia
West Asia	Bahrain, Iran, Israel, Kuwait, Oman, Qatar, Saudi Arabia, Turkey, United Arab Emirates, Rest of Western Asia, Jordan

672 **Table SM2.2:** Sectoral aggregation. The abbreviation *nec* stands for not elsewhere classified.

Sectors	Sub-sectors
Coal	Coal
Construction	Construction
Crops	Paddy rice, Wheat, Cereal grains nec, Vegetables, fruit, nuts, Oil seeds, Sugar cane, sugar beet, Plant-based fibers, Crops nec, Forestry
Crude oil	Oil
Electricity	Electricity
Food	Bovine meat products, Meat products nec, Vegetable oils and fats, Dairy products, Processed rice, Sugar, Food products nec, Beverages and tobacco products
Natural gas	Gas, Gas manufacture, distribution
Livestock	Bovine cattle, sheep and goats, horses, Animal products nec, Raw milk, Wool, silk-worm cocoons, Fishing
Manufacturing	Textiles, Wearing apparel, Leather products, Wood products, Paper products, publishing, Chemical, rubber, plastic products, Mineral products nec, Ferrous metals, Metals nec, Metal products, Motor vehicles and parts, Transport equipment nec, Electronic equipment, Machinery and equipment nec, Manufactures nec, NA
Oil refinery	Petroleum, coal products
Services	Water, Trade, Communication, Financial services nec, Business services nec, Recreational and other services, Public Administration, Defense, Education, Health, Dwellings, NA
Transport	Transport nec, Water transport, Air transport

SM3: Socio-economic projections

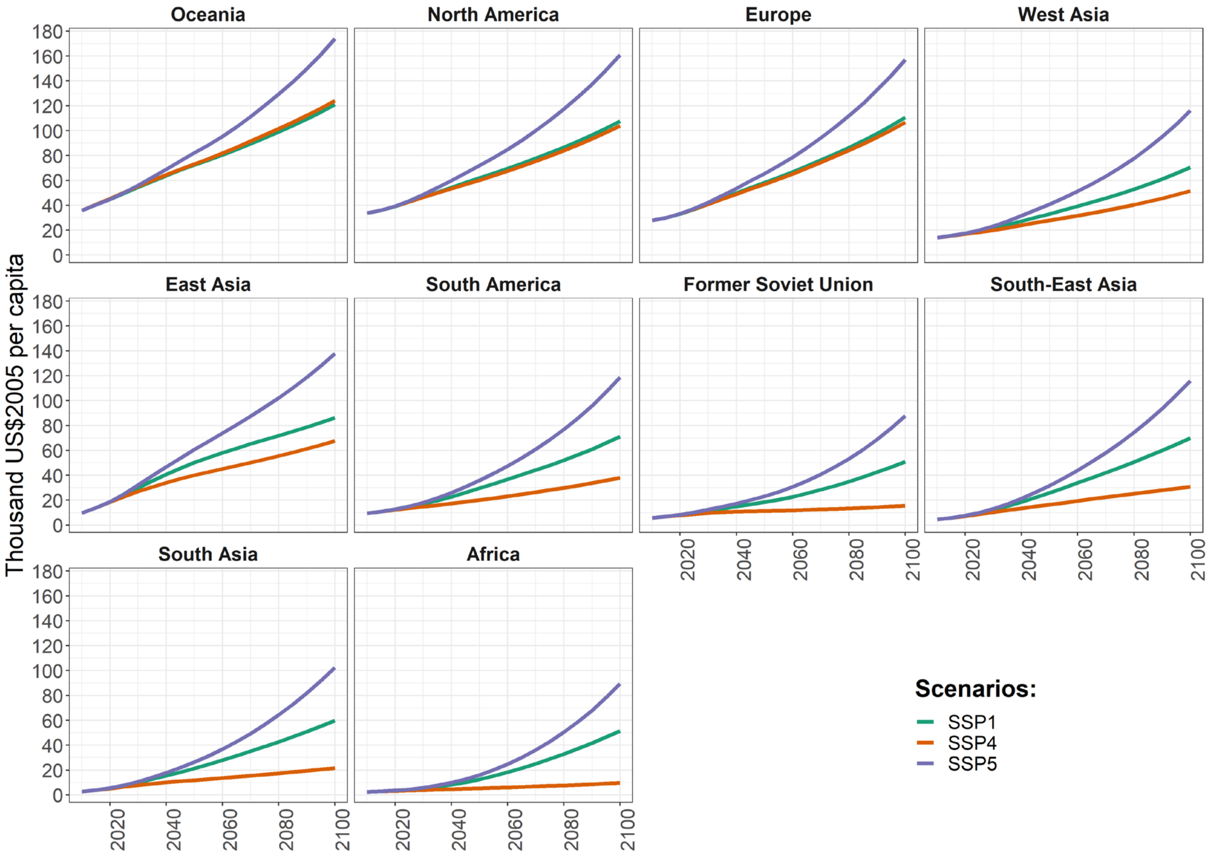

Fig. SM3.1: Projections of GDP per capita by region.

SM4: Income elasticities

Income elasticities of demand for non-agricultural goods and services are derived from the GTAP database. To estimate the income elasticities of demand for food products, we use the FAO and World Bank databases. Specifically, the FAO provides panel data on calories demand by country and year (see Fig. SM4.1). From the World Bank, we retrieve the time-series data on GDP per capita by country and year. The Lagrange multiplier test rejected the hull hypothesis, which implies that either a fixed effects or random effects model is appropriate (i.e., there are significant different among countries). A Hausman test suggested to use a fixed effects model because a random effects model turns out to be inconsistent. Therefore, we use a fixed effects regression to deal with a potential omitted variable bias, because apart from income there are other county-specific factors (i.e., individual-specific effects), which could affect the demand for food products.

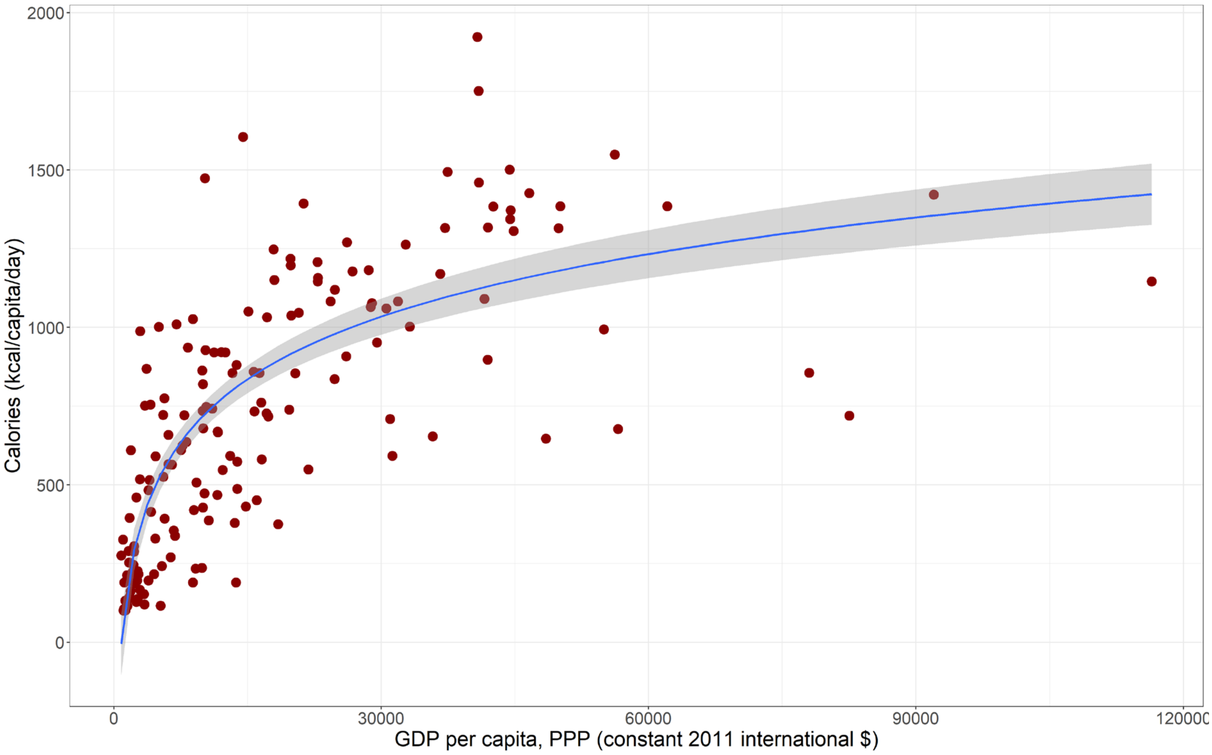

Fig. SM4.1: Demand for food products in calories and GDP per capita in 2011. Source: based on FAO and World Bank data.

To capture non-linearity in the relationship between calories consumption and income, we apply a level-log regression. Results from the fixed effects regression model are reported in Table SM4.1.

Table SM4.1: Fixed effects regression model.

ln(GDP/capita)	167.44^{***}
	(5.05)
R^2	0.23
Adj. R^2	0.20
Num. obs.	3838

$^{***}p < 0.001$, $^{**}p < 0.01$, $^{*}p < 0.05$

Income elasticities of demand for food are derived from the estimated regression model as follows.

$$C = \beta * \ln(GDP)$$

$$\frac{\partial C}{\partial GDP} = \frac{\beta}{GDP}$$

$$\frac{\partial C}{\partial GDP} * \frac{GDP}{C} = \frac{\beta}{GDP} * \frac{GDP}{C}$$

$$\epsilon = \frac{\beta}{C}$$

where *C* stands for calories consumption, *GDP* stands GDP per capital, β is the estimated coefficient (i.e., 166.38), and ϵ is the income elasticity of demand.

We assume that private consumption of unprocessed crops and livestock have the same values of income elasticities as the demand for food products. Using the estimated income elasticities of demand for food as well as the income elasticities of demand for other goods and services obtained from the GTAP database, we calculate levels of subsistence consumption for each demand category, which are scaled by population growth in dynamic model runs.

SM5: Sectoral productivity

Because production sectors are differently affected by HS to due to different heat exposure (e.g., agriculture vs. services), an accurate projection of structural changes is crucial for an economic impact assessment. Apart from consumption preferences, which can change over time in response to growing income, sectoral productivity is another important factor that drives a structural change. Empirical research reveals that factor productivity differs by sector. In our analysis, the calibration of total factor productivity (TFP) of sectors follows the approach implemented by Britz and Roson (2019). Specifically, TFP of services is endogenously determined in the reference scenario, and it becomes exogenous during simulations. TFP of agriculture and manufacturing is defined as $tfp_r * sh_{i,r,t}$:

$$sh_{i,r,t} = a + b * \frac{gdp_{r,t+1} - gdp_{r,t}}{gdp_{r,t}} + c * \left(\frac{gdp_{r,t+1} - gdp_{r,t}}{gdp_{r,t}}\right)^2$$

where tfp_r is the total factor productivity of services, $sh_{i,r,t}$ is the shift parameters for sector-specific productivity (i.e., agriculture and manufacturing), $gdp_{r,t}$ is the GDP per capital in region *r* in period *t*, and *a*, *b*, and *c* are the empirically estimated parameters for sector-specific productivity growth (see Table SM5.1) taken from the Britz and Roson (2019).

Table SM5.1: Estimated parameters for sector-specific productivity growth.

	Agriculture	Manufacturing
a	0.925391	2.893917
b	11.99205	-94.8599
c	291.8147	1680.554

Source: Britz and Roson (2019)

SM6: Mechanisation of outdoor jobs

To interpolate the relationship between GDP per capita and work intensity, we use a linear regression model. We consider a range of work intensity levels from 267 to 400 W. The agricultural sector in countries with the largest number of tractors is assumed to have a work intensity level of 267 W, whereas for countries with the lowest number of tractors, it is 400 W.

Table SM6.1: Regression results. The response variable is the level of work intensity, and the explanatory variable is GDP per capita.

(Intercept)	398.4717***
	(0.1721)
GDP/capita	-0.0007***
	(0.0000)
R^2	0.4180
Adj. R^2	0.4179
Num. obs.	5905

***$p < 0.001$, **$p < 0.01$, *$p < 0.05$

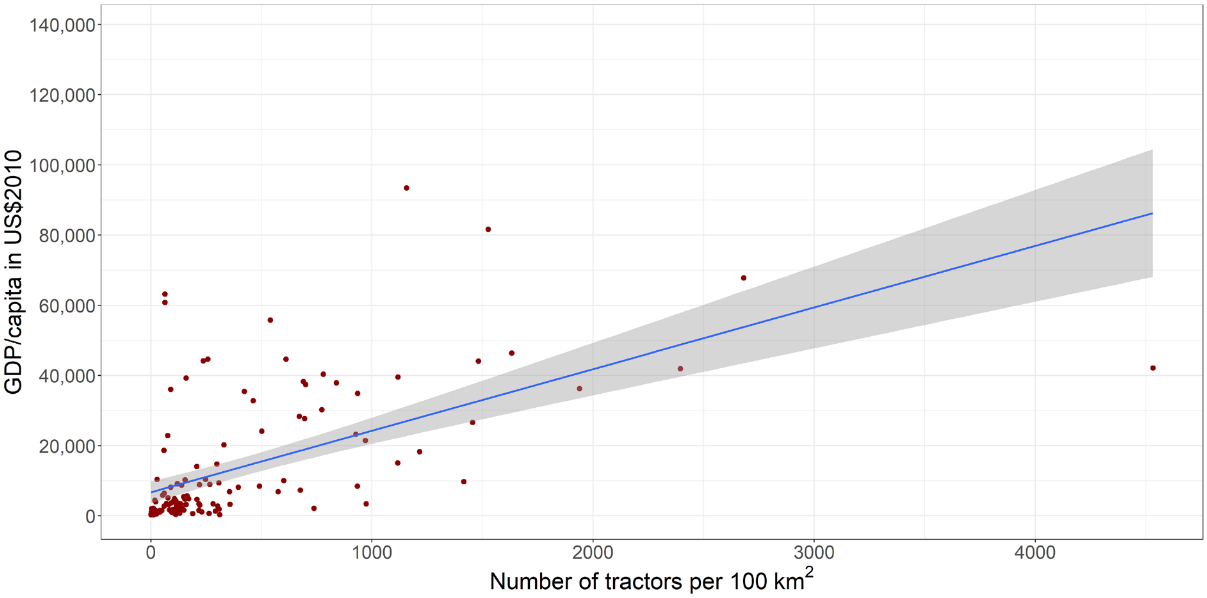

Fig. SM6.1: Relationship between income and mechanisation in agriculture in 2000. Based on the World Bank data.

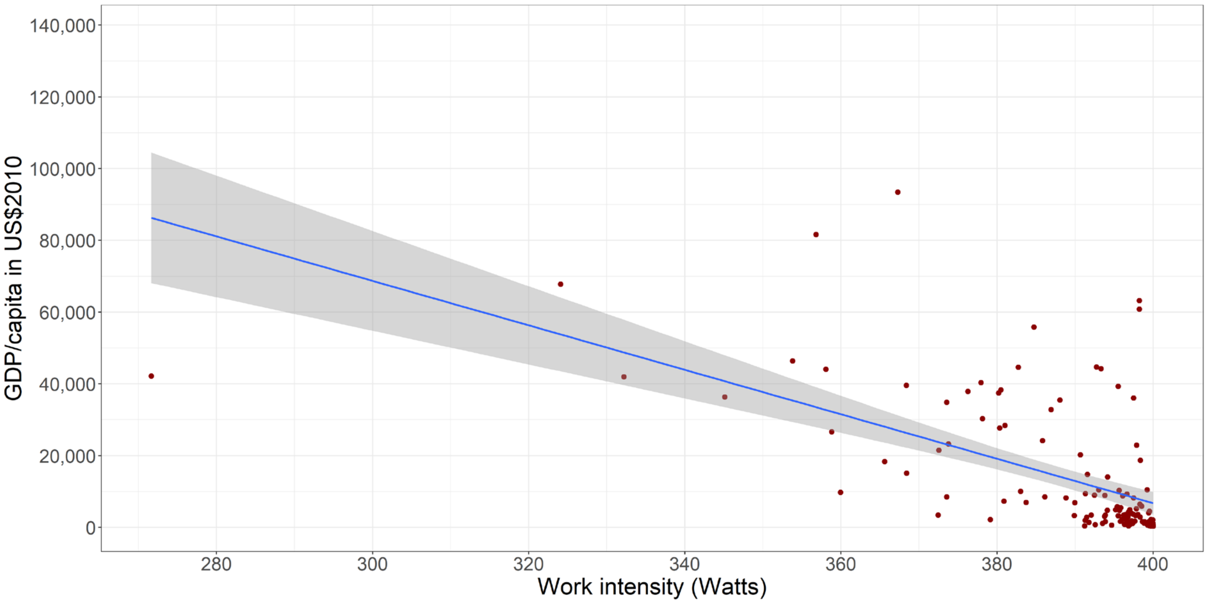

Fig. SM6.2: Interpolated relationship between income and work intensity in agriculture.

SM7: Supplementary results

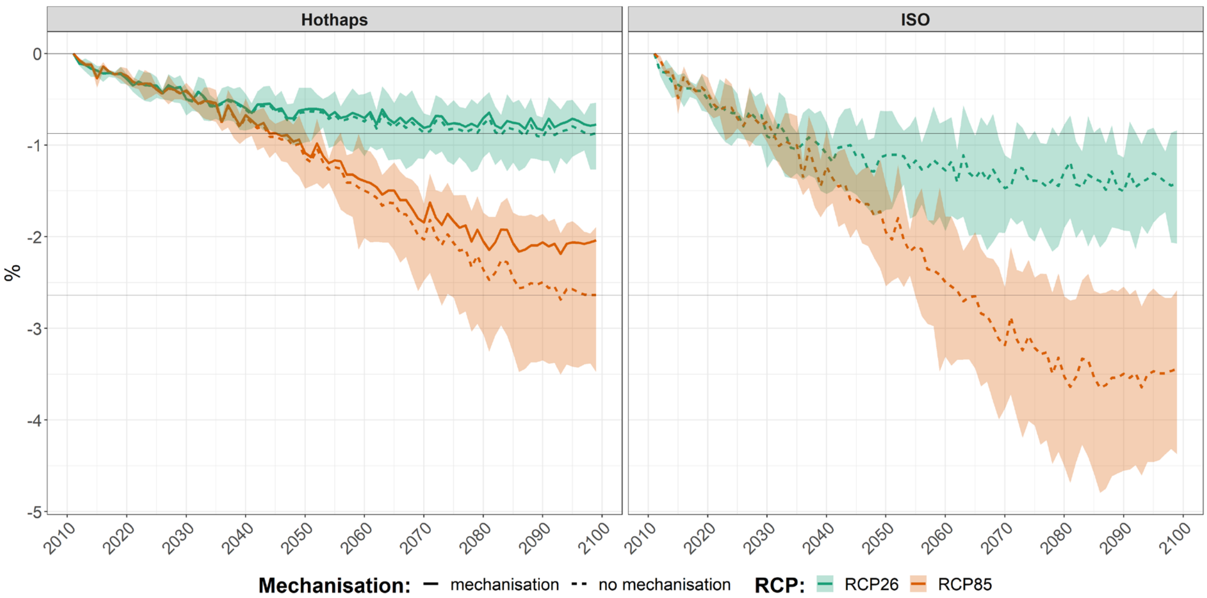

Fig. SM7.1: Changes in global private consumption under RCP2.6 and RCP8.5 compared to the reference scenario with no climate change. The solid and dashed lines show the mean values and the shaded areas indicate uncertainties of the estimated impacts. Mechanisation stands for decreasing work intensity through mechanisation driven by an economic growth. “Hothaps” stands for the epidemiological exposure-response function, while “ISO” implies that ISO: 7243:1989 standards are used to assess heat stress impacts on worker productivity.

The ANOVA analysis (see Fig. SM7.2) is conducted as follows. First, using the results from the GRACE model, we run a linear regression, where the response variable is relative changes in global GDP while explanatory variables are the categorical variables indicating the setting and parametrisation of model runs. We conduct the ANOVA analysis for four explanatory variables, such as climate models, labour mobility, RCPs, and substitution elasticities. The ANOVA analysis is then carried out on the obtained regression results. To calculate the proportions of variance explained, which indicates the relevance of variables, we use the incremental sums of squares from the ANOVA table.

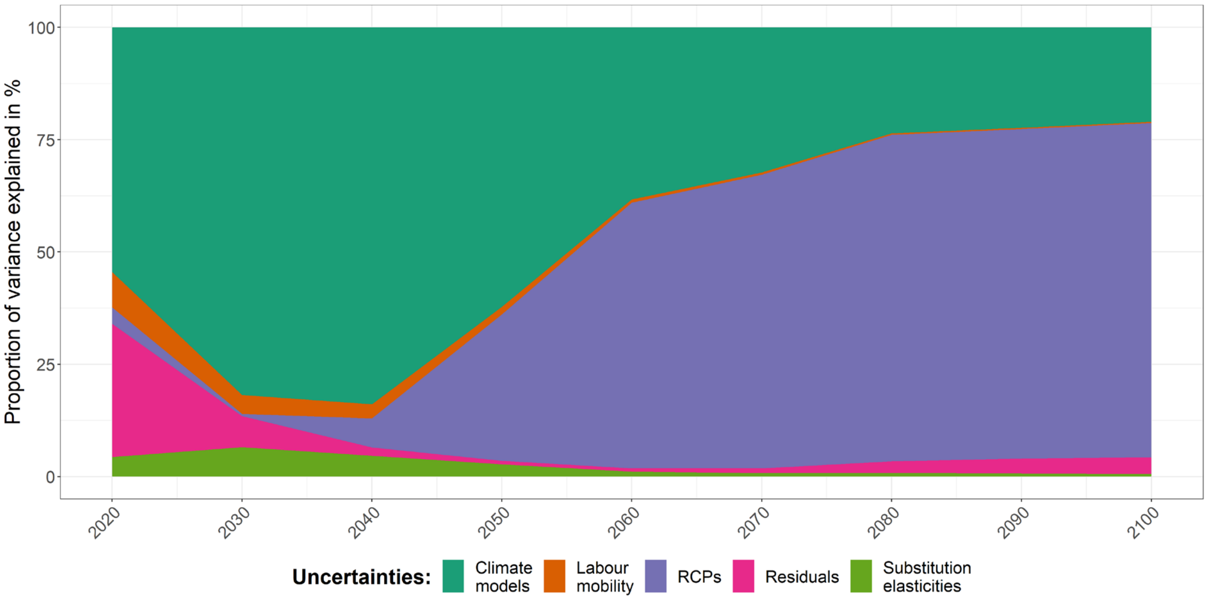

Fig. SM7.2: Analysis of variance for global GDP. The Hothaps function is used to estimate the heat impacts on worker productivity. The legend "Climate models" stands for the uncertainty of GCMs, "Labour mobility" is for the uncertainty of labour mobility (i.e., perfectly mobile vs. imperfectly mobile among sectors), "RCPs" is for the uncertainty of climate projects (i.e., RCP2.6 vs. RCP8.5), "Substitution elasticities" is for the uncertainty of substitution elasticities among primary factors (i.e., 0.3-0.7), and "Residuals" is for interactions terms.

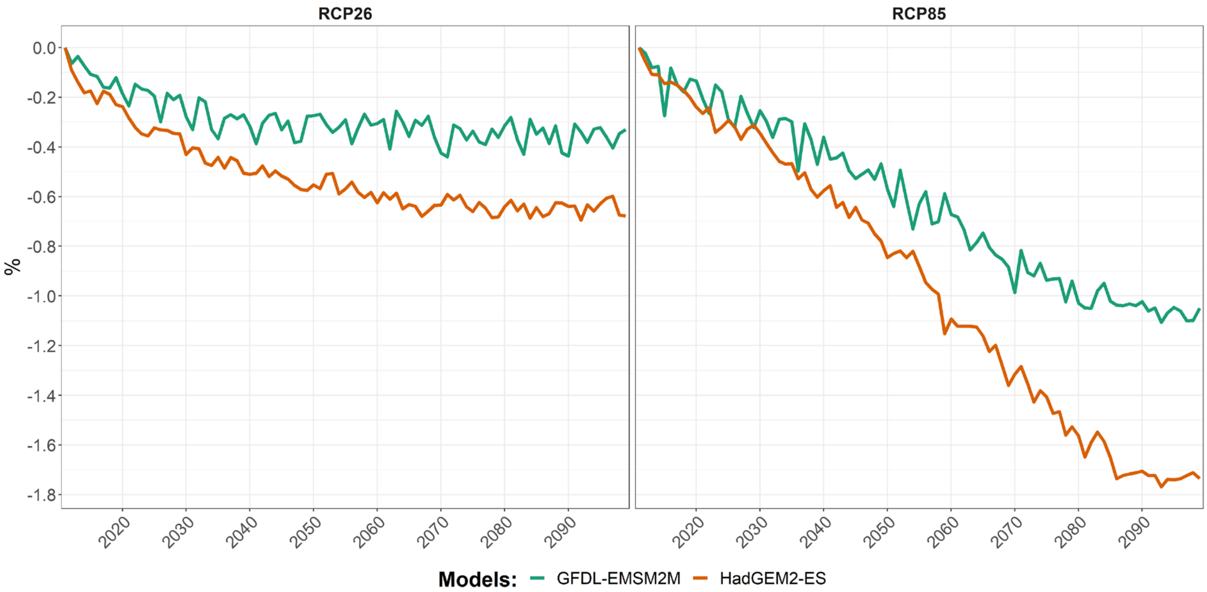

Fig. SM7.3: A model comparison of average changes in global GDP under RCP2.6 and RCP8.5 compared to the reference scenario with no climate change. The Hothaps function is used to estimate the heat impacts on worker productivity.

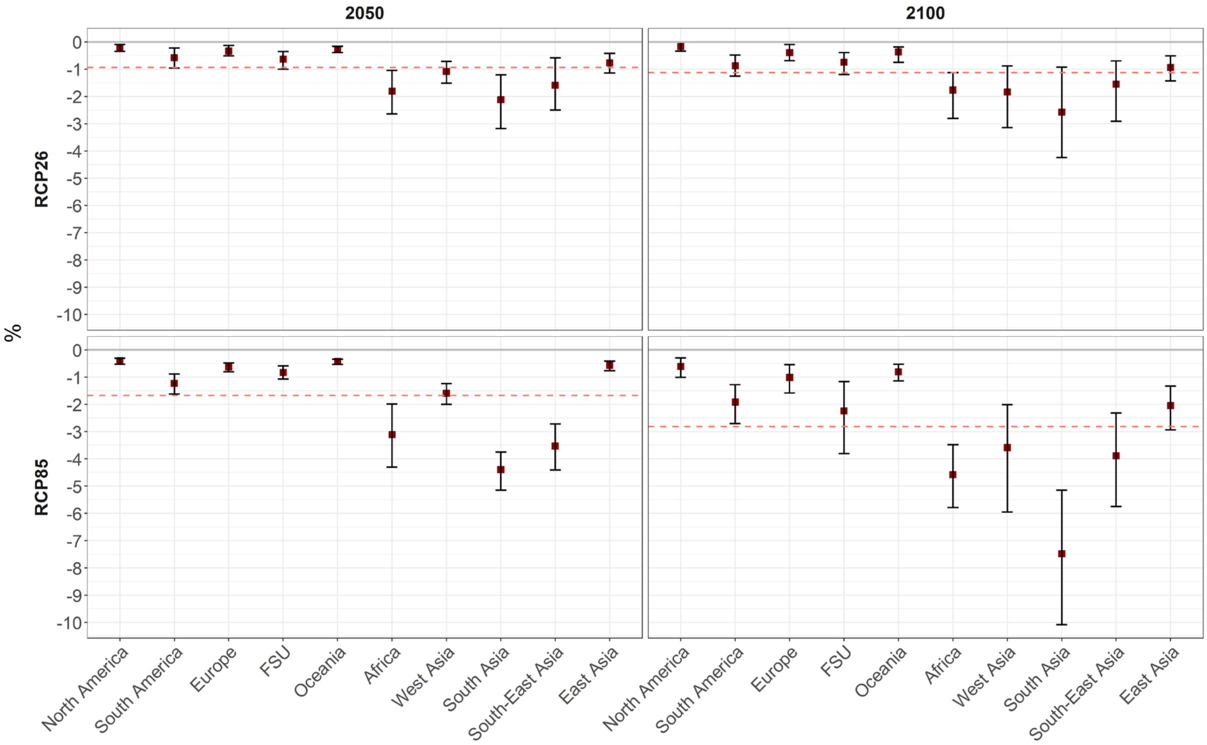

Fig. SM7.4: Changes in total private consumption by region under RCP2.6 and RCP8.5 by 2050 and 2100 compared to the reference scenario with no climate change. The Hothaps function is used to estimate the heat impacts on worker productivity. The error bars indicate the uncertainties around the estimates. The dashed read line shows unweighted average values across all regions, and the error bars indicate the uncertainties around the estimates.

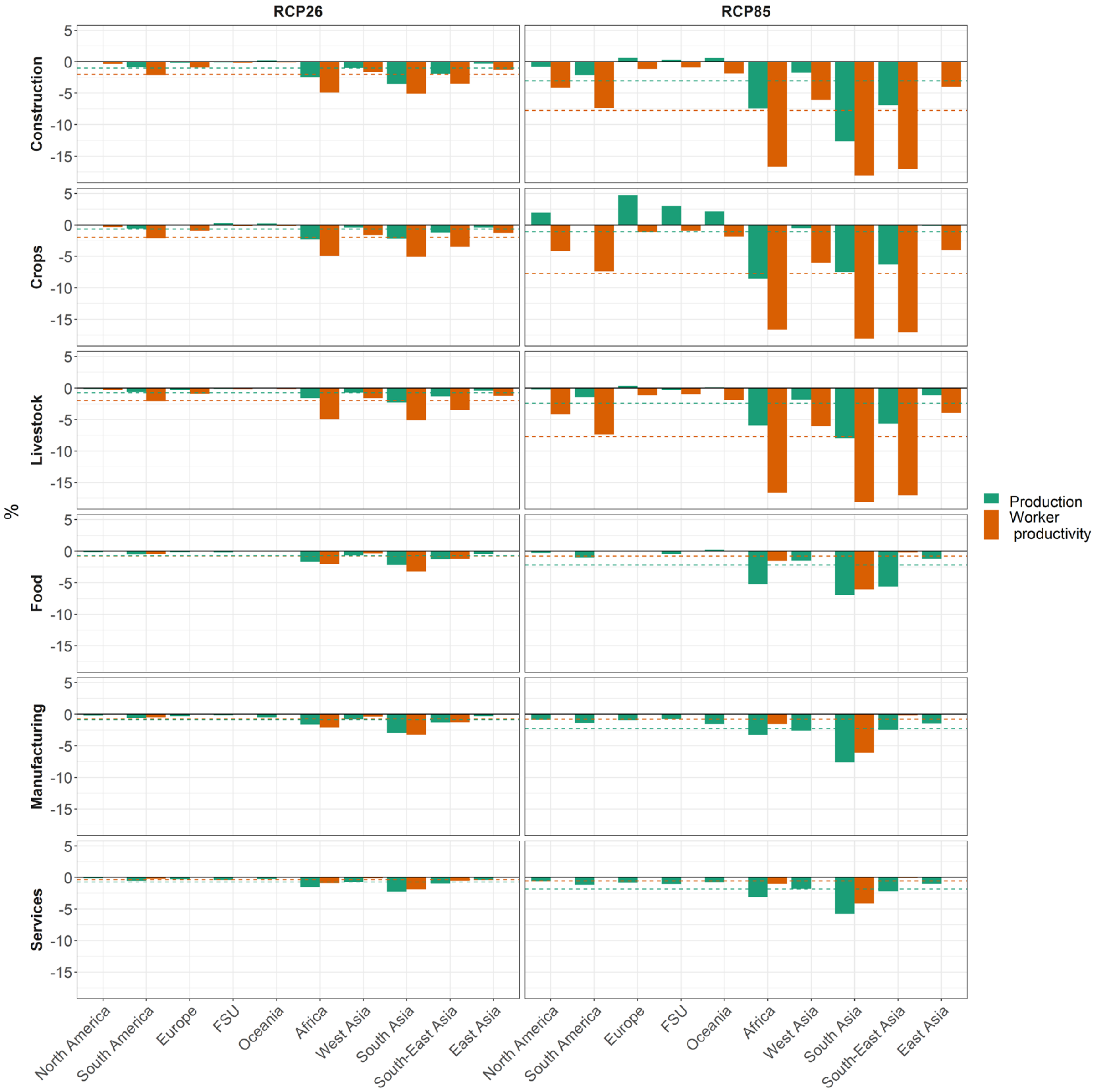

Fig. SM7.5: Average heat-induced changes in worker productivity and production by 2100 under RCP2.6 and RCP8.5 relative to the reference scenario with no climate change. The Hothaps function is used to estimate the heat impacts on worker productivity. The dashed lines show the mean values across regions.

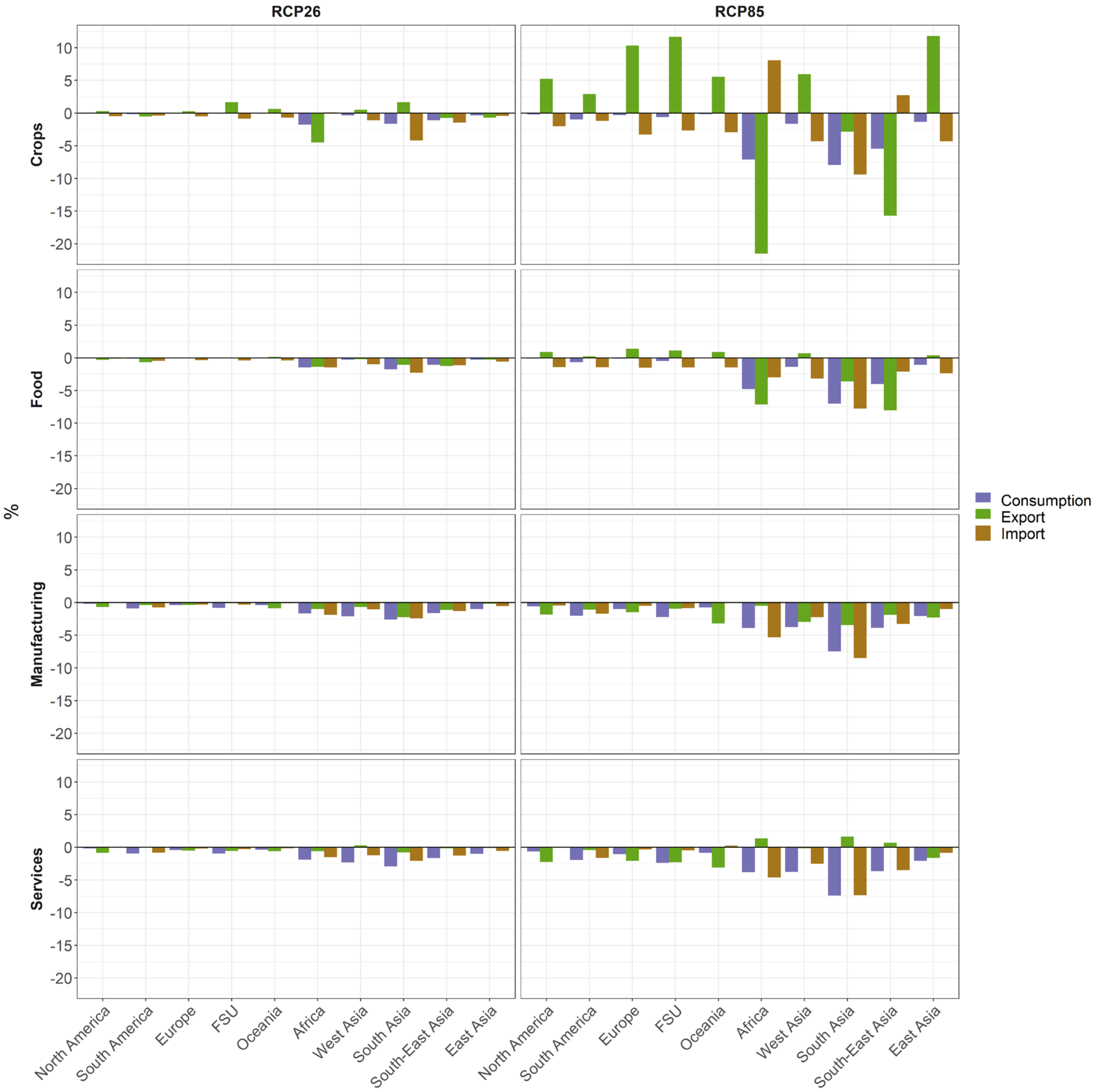

Fig. SM7.6: Average heat-induced changes in private consumption, exports, and imports by 2100 under RCP2.6 and RCP8.5 compared to the reference scenario with no climate change. The Hothaps function is used to estimate the heat impacts on worker productivity.

References

Aaheim, H.A., Orlov, A., Wei, T., Glomsrød, S., 2018. GRACE model and applications, CICERO Report 2018:01.

Ahmadalipour, A., Moradkhani, H., 2018. Escalating heat-stress mortality risk due to global warming in the Middle East and North Africa (MENA). Environ. Int. 117, 215–225. https://doi.org/10.1016/j.envint.2018.05.014

Akpinar-Ferrand, E., Singh, A., 2010. Modeling increased demand of energy for air conditioners and consequent CO2 emissions to minimize health risks due to climate change in India. Environ. Sci. Policy 13, 702–712. https://doi.org/10.1016/j.envsci.2010.09.009

Angel, A., Narayanan, B., McDougall, R., 2016. GTAP Data Bases: GTAP 9 Data Base Documentation [WWW Document]. URL https://www.gtap.agecon.purdue.edu/databases/v9/v9_doco.asp (accessed 12.14.17).

Basu, R., Samet, J.M., 2002. Relation between Elevated Ambient Temperature and Mortality: A Review of the Epidemiologic Evidence. Epidemiol. Rev. 24, 190–202. https://doi.org/10.1093/epirev/mxf007

Bernard, T.E., Pourmoghani, M., 1999. Prediction of workplace wet bulb global temperature. Appl. Occup. Environ. Hyg. 14, 126–134. https://doi.org/10.1080/104732299303296

Blois, J.D., Kjellstrom, T., Agewall, S., Ezekowitz, J.A., Armstrong, P.W., Atar, D., 2015. The Effects of Climate Change on Cardiac Health. Cardiology 131, 209–217. https://doi.org/10.1159/000398787

Britz, W., Roson, R., 2019. G-RDEM: A GTAP-Based Recursive Dynamic CGE Model for Long-Term Baseline Generation and Analysis. J. Glob. Econ. Anal. 4, 50–96.

Bröde, P., Fiala, D., Lemke, B., Kjellstrom, T., 2018. Estimated work ability in warm outdoor environments depends on the chosen heat stress assessment metric. Int. J. Biometeorol. 62, 331–345. https://doi.org/10.1007/s00484-017-1346-9

Calvin, K., Bond-Lamberty, B., Clarke, L., Edmonds, J., Eom, J., Hartin, C., Kim, S., Kyle, P., Link, R., Moss, R., McJeon, H., Patel, P., Smith, S., Waldhoff, S., Wise, M., 2017. The SSP4: A world of deepening inequality. Glob. Environ. Change 42, 284–296. https://doi.org/10.1016/j.gloenvcha.2016.06.010

Casanueva, A., 2019. HeatStress: Calculate heat stress indices. R package version 1.0.6.

Château, J., Dellink, R., Lanzi, E., 2014. An Overview of the OECD ENV-Linkages Model.

CIESIN, (Center for International Earth Science Information Network - CIESIN - Columbia University), 2017. Gridded Population of the World, Version 4 (GPWv4): Population Count Adjusted to Match 2015 Revision of UN WPP Country Totals, Revision 10.

Corong, E.L., Hertel, T.W., McDougall, R., Tsigas, M.E., Mensbrugghe, D. van der, 2017. The Standard GTAP Model, Version 7. J. Glob. Econ. Anal. 2, 1–119. https://doi.org/10.21642/JGEA.020101AF

DARA, 2012. DARA; Climate Vulnerable Forum. 2012. Climate Vulnerability Monitor, 2nd edition: A guide to the cold calculus of a hot plaent (DARA). URL https://daraint.org/climate-vulnerability-monitor/climate-vulnerability-monitor-2012/report/ (accessed 7.16.19).

Dixon, P.B., Rimmer, M.T., 2006. The Displacement Effect of Labour-Market Programs: MONASH Analysis*. Econ. Rec. 82, S26–S40. https://doi.org/10.1111/j.1475-4932.2006.00330.x

Dosio, A., Mentaschi, L., Fischer, E.M., Wyser, K., 2018. Extreme heat waves under 1.5\hspace0.167em°C and 2\hspace0.167em°C global warming. Environ. Res. Lett. 13, 054006. https://doi.org/10.1088/1748-9326/aab827

Dunne, J.P., Stouffer, R.J., John, J.G., 2013. Reductions in labour capacity from heat stress under climate warming. Nat. Clim. Change 3, 563–566. https://doi.org/10.1038/nclimate1827

Gasparrini, A., Guo, Y., Sera, F., Vicedo-Cabrera, A.M., Huber, V., Tong, S., de Sousa Zanotti Stagliorio Coelho, M., Nascimento Saldiva, P.H., Lavigne, E., Matus Correa, P., Valdes Ortega, N., Kan, H., Osorio, S., Kyselý, J., Urban, A., Jaakkola, J.J.K., Ryti, N.R.I., Pascal, M., Goodman, P.G., Zeka, A., Michelozzi, P., Scortichini, M., Hashizume, M., Honda, Y., Hurtado-Diaz, M., Cesar Cruz, J., Seposo, X., Kim, H., Tobias, A., Iñiguez, C., Forsberg, B., Åström, D.O., Ragettli, M.S., Guo, Y.L., Wu, C., Zanobetti, A., Schwartz, J., Bell, M.L., Dang, T.N., Van, D.D., Heaviside, C., Vardoulakis, S., Hajat, S., Haines, A., Armstrong, B., 2017. Projections of temperature-related excess mortality under climate change scenarios. Lancet Planet. Health 1, e360–e367. https://doi.org/10.1016/S2542-5196(17)30156-0

Hajat, S., Kosatsky, T., 2010. Heat-related mortality: a review and exploration of heterogeneity. J. Epidemiol. Community Health 64, 753–760. https://doi.org/10.1136/jech.2009.087999

Hempel, S., Frieler, K., Warszawski, L., Schewe, J., Piontek, F., 2013. A trend-preserving bias correction – the ISI-MIP approach. Earth Syst. Dyn. 4, 219–236. https://doi.org/10.5194/esd-4-219-2013

Hertel, T., Mensbrugghe, D. van der, 2016. Chapter 14: Behavioral Parameters [WWW Document]. Cent. Glob. Trade Anal. URL http://www.gtap.agecon.purdue.edu/resources/res_display.asp?RecordID=5138

Hsiang, S., Kopp, R., Jina, A., Delgado, M., Rising, J., Mohan, S., Muir-Wood, R., Rasmussen, D.J., Wilson, P., Larsen, K., Houser, T., 2014. American Climate Prospectus: Economic Risks in the United States. Clim. Impact Lab. URL http://www.impactlab.org/research/american-climate-prospectus/ (accessed 7.17.19).

IPCC, 2014. AR5 Climate Change 2014: Mitigation of Climate Change — IPCC. URL https://www.ipcc.ch/report/ar5/wg3/ (accessed 5.22.19).

Isaac, M., van Vuuren, D.P., 2009. Modeling global residential sector energy demand for heating and air conditioning in the context of climate change. Energy Policy 37, 507–521. https://doi.org/10.1016/j.enpol.2008.09.051

ISO, 1989. Hot environments — Estimation of the heat stress on working man, based on the WBGT-index (wet bulb globe temperature). ISO Standard 7243. Geneva: International Standards Organization; 1989.

Jones, B., O'Neill, B.C., 2016. Spatially explicit global population scenarios consistent with the Shared Socioeconomic Pathways. Environ. Res. Lett. 11, 084003. https://doi.org/10.1088/1748-9326/11/8/084003

Kjellstrom, T., Briggs, D., Freyberg, C., Lemke, B., Otto, M., Hyatt, O., 2016. Heat, Human Performance, and Occupational Health: A Key Issue for the Assessment of Global Climate Change Impacts. Annu. Rev. Public Health 37, 97–112. https://doi.org/10.1146/annurev-publhealth-032315-021740

Kjellstrom, T., Freyberg, C., Lemke, B., Otto, M., Briggs, D., 2018. Estimating population heat exposure and impacts on working people in conjunction with climate change. Int. J. Biometeorol. 62, 291–306. https://doi.org/10.1007/s00484-017-1407-0

Kjellstrom, T., Holmer, I., Lemke, B., 2009. Workplace heat stress, health and productivity – an increasing challenge for low and middle-income countries during climate change. Glob. Health Action 2. https://doi.org/10.3402/gha.v2i0.2047

Kjellstrom, T., Maitre, N., Saget, C., Otto, M., Karimova, T., 2019. Working on a warmer planet: The effect of heat stress on productivity and decent work (Report).

Kovats, R.S., Hajat, S., 2008. Heat Stress and Public Health: A Critical Review. Annu. Rev. Public Health 29, 41–55. https://doi.org/10.1146/annurev.publhealth.29.020907.090843

Lemke, B., Kjellstrom, T., 2012. Calculating Workplace WBGT from Meteorological Data: A Tool for Climate Change Assessment. Ind. Health 50, 267–278. https://doi.org/10.2486/indhealth.MS1352

Liljegren, J.C., Carhart, R.A., Lawday, P., Tschopp, S., Sharp, R., 2008. Modeling the wet bulb globe temperature using standard meteorological measurements. J. Occup. Environ. Hyg. 5, 645–655. https://doi.org/10.1080/15459620802310770

Ma, R., Zhong, S., Morabito, M., Hajat, S., Xu, Z., He, Y., Bao, J., Sheng, R., Li, C., Fu, C., Huang, C., 2019. Estimation of work-related injury and economic burden attributable to heat stress in Guangzhou, China. Sci. Total Environ. 666, 147–154. https://doi.org/10.1016/j.scitotenv.2019.02.201

McNeil, M.A., Letschert, V.E., 2008. Future Air Conditioning Energy Consumption in Developing Countries and what can be done about it: The Potential of Efficiency in the Residential Sector.

Meehl, G.A., Tebaldi, C., 2004. More Intense, More Frequent, and Longer Lasting Heat Waves in the 21st Century. Science 305, 994–997. https://doi.org/10.1126/science.1098704

Orlov, A., Sillmann, J., Aaheim, A., Aunan, K., de Bruin, K., 2019. Economic Losses of Heat-Induced Reductions in Outdoor Worker Productivity: a Case Study of Europe. Econ. Disasters Clim. Change. https://doi.org/10.1007/s41885-019-00044-0

Parsons, K., 2014. Human Thermal Environments: The Effects of Hot, Moderate, and Cold Environments on Human Health, Comfort, and Performance. CRC Press, Inc.

Phung, D., Thai, P.K., Guo, Y., Morawska, L., Rutherford, S., Chu, C., 2016. Ambient temperature and risk of cardiovascular hospitalization: An updated systematic review and meta-analysis. Sci. Total Environ. 550, 1084–1102. https://doi.org/10.1016/j.scitotenv.2016.01.154

Poulianiti, K.P., Havenith, G., Flouris, A.D., 2019. Metabolic energy cost of workers in agriculture, construction, manufacturing, tourism, and transportation industries. Ind. Health 57, 283–305. https://doi.org/10.2486/indhealth.2018-0075

Riahi, K., van Vuuren, D.P., Kriegler, E., Edmonds, J., O'Neill, B.C., Fujimori, S., Bauer, N., Calvin, K., Dellink, R., Fricko, O., Lutz, W., Popp, A., Cuaresma, J.C., Kc, S., Leimbach, M., Jiang, L., Kram, T., Rao, S., Emmerling, J., Ebi, K., Hasegawa, T., Havlik, P., Humpenöder, F., Da Silva, L.A., Smith, S., Stehfest, E., Bosetti, V., Eom, J., Gernaat, D., Masui, T., Rogelj, J., Strefler, J., Drouet, L., Krey, V., Luderer, G., Harmsen, M., Takahashi, K., Baumstark, L., Doelman, J.C., Kainuma, M., Klimont, Z., Marangoni, G., Lotze-Campen, H., Obersteiner, M., Tabeau, A., Tavoni, M., 2017. The Shared Socioeconomic Pathways and their energy, land use, and greenhouse gas emissions implications: An overview. Glob. Environ. Change 42, 153–168. https://doi.org/10.1016/j.gloenvcha.2016.05.009

Roson, R., Sartori, M., 2016. Estimation of Climate Change Damage Functions for 140 Regions in the GTAP 9 Data Base. J. Glob. Econ. Anal. 1, 78–115. https://doi.org/10.21642/JGEA.010202AF

Roson, R., van der Mensbrugghe, D., 2012. Climate change and economic growth: impacts and interactions: International Journal of Sustainable Economy: Vol 4, No 3 [WWW Document]. URL https://www.inderscienceonline.com/doi/abs/10.1504/IJSE.2012.047933 (accessed 9.19.19).

Russo, S., Sillmann, J., Sterl, A., 2017. Humid heat waves at different warming levels. Sci. Rep. 7, 7477. https://doi.org/10.1038/s41598-017-07536-7

Sahu, S., Sett, M., Kjellstrom, T., 2013. Heat exposure, cardiovascular stress and work productivity in rice harvesters in India: implications for a climate change future. Ind. Health 51, 424–431.

Takakura, J., Fujimori, S., Takahashi, K., Hasegawa, T., Honda, Y., Hanasaki, N., Hijioka, Y., Masui, T., 2018. Limited Role of Working Time Shift in Offsetting the Increasing Occupational-Health Cost of Heat Exposure. Earths Future 6, 1588–1602. https://doi.org/10.1029/2018EF000883

Takakura, J., Fujimori, S., Takahashi, K., Hijioka, Y., Hasegawa, T., Honda, Y., Masui, T., 2017. Cost of preventing workplace heat-related illness through worker breaks and the benefit of climate-change mitigation. Environ. Res. Lett. 12, 064010. https://doi.org/10.1088/1748-9326/aa72cc

Tawatsupa, B., Yiengprugsawan, V., Kjellstrom, T., Berecki-Gisolf, J., Seubsman, S.-A., Sleigh, A., 2013. Association between Heat Stress and Occupational Injury among Thai Workers: Findings of the Thai Cohort Study. Ind. Health 51, 34–46. https://doi.org/10.2486/indhealth.2012-0138

Turner, L., Barnett, A., Connell, D., Tong, S., 2012. Ambient Temperature and Cardiorespiratory Morbidity: A Systematic Review and Meta-analysis. Epidemiology 23, 594–606. https://doi.org/10.1097/EDE.0b013e3182572795
Warszawski, L., Frieler, K., Huber, V., Piontek, F., Serdeczny, O., Schewe, J., 2014. The Inter-Sectoral Impact Model Intercomparison Project (ISI–MIP): Project framework. Proc. Natl. Acad. Sci. 111, 3228–3232. https://doi.org/10.1073/pnas.1312330110
World Bank, 2019. World Development Indicators. Agricultural machinery, tractors per 100 sq. km of arable land.
Wyndham, C.H., 1969. Adaptation to heat and cold. Environ. Res. 2, 442–469.